

Band Gap Optimization of In-Plane Mode Phononic Crystal by Dispersion Tuning



Scholar Name: Bushra Iram

Scholar ID: 19030-D

Program: MPhil Physics

Department of Physics & Numerical Science

Date of submission: _____

Supervisor: Dr. Muhammad Ammar Khan

**Qurtuba University of Science & Information Technology
D.I. Khan, Khyber Pakhtunkhwa, Pakistan**

THESIS SUBMISSION CERTIFICATE BY SUPERVISOR

This is to certify that the thesis submitted by

Scholar's Name: Bushra Iram

Scholar's ID # 19030-D

is of sufficient merit to justify its acceptance by
Department of Physical and Numerical Sciences

Qurtuba University of Science and Information Technology,
D.I. Khan

for the award of a Degree of
Program: MPhil Physics

I recommend that the thesis/dissertation be accepted for the award of the
degree of M. Phil.

Supervisor: Dr. Muhammad Ammar Khan

(Signature)

Author's Declaration

I hereby declare that this thesis neither as a whole nor a part thereof has been copied from any source. It is further declared that I have developed this thesis on the basis of my personal efforts made under the guidance of my supervisor. No portion of the work presented in this thesis has been submitted in support of any other degree or qualification of this or any other University or Institute of learning, if found I shall stand responsible.

Signature:_____

Acknowledgements

In the name of ALLAH, the Merciful, the compassionate all praise is due to ALLAH, the Lord of the Worlds. He bestowed His favors abundantly on us. I bear witness that there is no deity save ALLAH, having no associates. All the praise and thanks are due to Him. I also bear witness that Prophet MUHAMMAD (SAW) is the Messenger of ALLAH. May the peace and blessings of ALLAH be upon him, His pure grateful family and companions, and all those who follow them in righteousness till the Day of Judgment. Extending gratitude of thanks to my respected supervisor, Dr. Muhammad Ammar khan, who always steps forward to support and guide me. He is so polite and nice throughout the project. He always guided me on the right path and taught me how to move forward. How can I forget to thanks to my dear parents and husband who are always with me in every ups and downs of my life, they never let me down in any stage of my life.

Finally, my warm wishes and prayers for those who helped me in finalizing my thesis. May Almighty ALLAH bless all, Ameen.

Table of Contents

| | |
|--------------------------------------------------------|------|
| Author's Declaration..... | ii |
| Acknowledgements..... | iii |
| Table of Contents..... | iv |
| List of Figures | vi |
| List of Tables | viii |
| ABSTRACT..... | ix |
| CHAPTER 1 | 1 |
| Introduction..... | 1 |
| 1.1 Overview..... | 1 |
| 1.2 Background of Study | 1 |
| 1.3 Types of Phononic Crystals | 3 |
| 1.3.1 Acoustic phononic crystals /metamaterials..... | 3 |
| 1.3.2 Elastic phononic crystals / metamaterials | 4 |
| 1.4 Phononic crystals resonator | 6 |
| 1.5 Phononic Crystals and Thermal Effect | 6 |
| 1.6 Dynamics of Phononic Structures and Materials..... | 7 |
| 1.7 Band gap and phononic crystal | 7 |
| 1.10 Problem Statement | 9 |
| 1.11 Aims and Objectives | 9 |
| 1.12 Significance & Scope of Study | 9 |
| 1.13 Definitions Of Key Terms Of The Study | 10 |
| 1.13.1 Phononic Crystal | 10 |
| 1.13.2 Microelectromechanical system..... | 10 |

| | |
|--------------------------------------------|-----------|
| 1.13.3 Dispersion tunning | 10 |
| 1.13.5 Surface acoustic wave..... | 11 |
| 1.13.6 Electromagnetic material | 11 |
| 1.13.7 Mechanical waves..... | 11 |
| 1.14 Advantages of phononic crystal..... | 11 |
| 1.15 Disadvanges of phononic crystal | 12 |
| CHAPTER 2 | 13 |
| LITERATURE REVIEW | 13 |
| CHAPTER 3 | 28 |
| Research Methodology | 28 |
| 3.1 Silicon Carbide..... | 31 |
| 3.2 Silicon Nitride..... | 32 |
| 3.3 Indium Antimonide | 34 |
| CHAPTER 4 | 37 |
| Results & Discussion | 37 |
| CHAPTER 5 | 49 |
| Conclusion & Future Work..... | 49 |
| 5.1 Future work And Applications..... | 49 |
| References | 51 |

List of Figures

| | |
|----------------------------------------------------------------------------------------------------------------------------------------------------------------------------------------------------------------------------------------------------------------------------------------------------|----|
| Figure 1.1:A unit cell of a typical acoustic metamaterial plate: (a) front view; (b) perspective view[6]. | 4 |
| Figure 1.2:Dispersion surfaces and band gap of the above metamaterial: (a) dispersion surfaces; (b) stopband (gray rectangle) [6]. | 4 |
| Figure1.3:Elastic metamaterials with hexagonal unit cells: (a) primitive cell; (b) Brillouin zone; (c) band structures around the boundaries of the irreducible Brillouin zone [7]..... | 5 |
| Figure 2.1:A schematic illustration of a two-dimensional square–pillar-type phononic crystal (PnC) with decoupled double defects..... | 18 |
| Figure 2.2: Shows the graphical representation of dynamic directional amplifier(DDA). | 21 |
| Figure 2.3:Proposal of conceptual metastructure design (a) view of 3 dimension(b) dynamic directional amplifier (DDA) components. | 21 |
| Figure 2.4:(a)Mechanically tunable graphene structure (b) Density of states calculated from the finite model as a function of pressure applied to the suspended PnC[48].calculated from the finite model as a function of pressure applied to the suspended PnC ($T_0 = 0.010 \text{ N/m}$)..... | 25 |
| Figure 3.1:phononic crystal unit cell $4\mu\text{m} \times 4\mu\text{m}$ and chamfer vertex is $0.2\mu\text{m}$ | 29 |
| Figure 3.2:Mesh of proposed phononic crystal with sharp edges, and irreducible Brillouin zone of PnC for k parametric sweeping. | 30 |
| Figure 3.3:Schematic diagram of a Silicon carbide PnC cell with lattice parameter $a = 4\mu\text{m}$, and Supercell model consisting of 4×4 cells with $1.2 \mu\text{m}$ diameter hole. | 31 |
| Figure 3.4:Schematic diagram of a Silicon carbide PnC cell with lattice parameter $a = 4\mu\text{m}$, and Supercell model consisting of 4×4 cells with $1.4 \mu\text{m}$ diameter hole. | 31 |
| Figure3.5:Schematic diagram of a Silicon carbide PnC cell with lattice parameter $a = 4\mu\text{m}$, and Supercell model consisting of 4×4 cells with $1.6 \mu\text{m}$ diameter hole. | 32 |
| Figure 3.6:Schematic diagram of a Silicon Nitride PnC cell with lattice parameter $a = 4\mu\text{m}$, and Supercell model consisting of 4×4 cells with $1.2 \mu\text{m}$ diameter hole. | 33 |
| Figure 3.7:Schematic diagram of a Silicon Nitride PnC cell with lattice parameter $a = 4\mu\text{m}$, and Supercell model consisting of 4×4 cells with $1.4 \mu\text{m}$ diameter hole. | 33 |
| Figure 3.8:Schematic diagram of a Silicon Nitride PnC cell with lattice parameter $a = 4\mu\text{m}$, and Supercell model consisting of 4×4 cells with $1.6 \mu\text{m}$ diameter hole | 34 |
| Figure 3.9:Schematic diagram of a Indium Antimonide PnC cell with lattice parameter $a = 4\mu\text{m}$, and Supercell model consisting of 4×4 cells with $1.2 \mu\text{m}$ diameter hole. | 35 |
| Figure 3.10:Schematic diagram of a Indium Antimonide PnC cell with lattice parameter $a = 4\mu\text{m}$, and | |

| | |
|-------------------------------------------------------------------------------------------------------------------------------------------------------------------------------------------------------------|----|
| Supercell model consisting of 4×4 cells with $1.4 \mu\text{m}$ diameter hole..... | 35 |
| Figure 3.11:Schematic diagram of a Indium Antimonide PnC cell with lattice parameter $a = 4\mu\text{m}$, and Supercell model consisting of 4×4 cells with $1.6 \mu\text{m}$ diameter hole..... | 35 |
| Figure 4.1:Illustration of bands and dispersion relations of phononic crystal with chamfer corner..... | 38 |
| Figure 4.2:Dispersion curves and band structure of Silicon Carbide with $r=0.6\mu\text{m}$ hole..... | 38 |
| Figure 4.3:The eigenmode shapes of the first 4 frequency bands of the proposed PnC of Silicon Carbide with $r=0.6\mu\text{m}$ hole..... | 39 |
| Figure 4.4:Dispersion curves and band structure of Silicon Carbide with $r=0.7\mu\text{m}$ hole..... | 39 |
| Figure 4.5:The eigenmode shapes of the first 4 frequency bands of the proposed PnC of Silicon Carbide with $r=0.7\mu\text{m}$ hole..... | 40 |
| Figure 4.6:Dispersion curves and band structure of Silicon Carbide with $r=0.8\mu\text{m}$ hole..... | 40 |
| Figure 4.7:The eigenmode shapes of the first 4 frequency bands of the proposed PnC of Silicon Carbide with $r=0.8\mu\text{m}$ hole..... | 41 |
| Figure 4.8:Dispersion curves and band structure of Silicon Nitride with $r=0.6\mu\text{m}$ hole | 41 |
| Figure 4.9:The eigenmode shapes of the first 4 frequency bands of the proposed PnC of Silicon Nitride with $r=0.6\mu\text{m}$ hole..... | 42 |
| Figure 4.10:Dispersion curves and band structure of Silicon Nitride with $r=0.7\mu\text{m}$ hole | 42 |
| Figure 4.11:The eigenmode shapes of the first 4 frequency bands of the proposed PnC of Silicon Nitride with $r=0.7\mu\text{m}$ hole..... | 43 |
| Figure 4.12:Dispersion curves and band structure of Silicon Nitride with $r=0.8\mu\text{m}$ hole | 43 |
| Figure 4.13:The eigenmode shapes of the first 4 frequency bands of the proposed PnC of Silicon Nitride with $r=0.8\mu\text{m}$ hole..... | 44 |
| Figure 4.14:Dispersion curves and band structure of Indium antimonide with $r=0.6\mu\text{m}$ hole | 44 |
| Figure 4.15:The eigenmode shapes of the first 4 frequency bands of the proposed PnC of Indium antimonide with $r=0.6\mu\text{m}$ hole..... | 45 |
| Figure 4.16:Dispersion curves and band structure of Indium antimonide with $r=0.7\mu\text{m}$ hole | 45 |
| Figure 4.17:The eigenmode shapes of the first 4 frequency bands of the proposed PnC of Indium antimonide with $r=0.7\mu\text{m}$ hole..... | 46 |
| Figure 4.18:Dispersion curves and band structure of Indium antimonide with $r=0.8\mu\text{m}$ hole | 46 |
| Figure 4.19:The eigenmode shapes of the first 4 frequency bands of the proposed PnC of Indium antimonide with $r=0.8\mu\text{m}$ hole..... | 47 |
| Figure 4.20:Illustration of band gaps of three materials with air hole inclusion of radium $0.7\mu\text{m}$ and $0.8\mu\text{m}$ | 48 |

List of Tables

| | |
|-----------------------------------------------------------------------------------------------|----|
| Table 2.1:shows design, material, and band gap frequency. | 27 |
| Table 3.1:Properties of materials (SiC (6H) - Silicon carbide) used in the PnC structure..... | 32 |
| Table 3.2:Properties of materials (Silicon Nitride) used in the PnC structure. | 34 |
| Table 3.3:Properties of materials (Indium Antimonide) used in the PnC structure | 36 |
| Table 4.1: Upper and Lower frequency bands limits of three materials. | 48 |

ABSTRACT

This research presents a novel approach for optimization of band gap and dispersion relation of In-plane mode two dimensional Phononic crystal. In this work a new design of phononic crystal is designed and the propagation of acoustic/elastic waves in two dimensional phononic crystals (PnC) is studied theoretically through periodic boundary Finite Element Analysis (FEA) simulation. Analyzed band structure show that forbidden bands and pass bands can be change by changing the radius of air inclusion hole of phononic crystal. The variation of absolute bandgap of PnC is investigated as a function of air inclusion in material as well as the property of that material. Initially PnC unit cell designed with dimension $4\mu\text{m} \times 4\mu\text{m}$ which consist of chamfer edges, and then modified to sharp edges with varying air inclusion hole in center. Vibrational waves displacement and dispersion curves is analyzed for 4×4 array of PnCs with radius of $0.6\mu\text{m}$, $0.7\mu\text{m}$, and $0.8\mu\text{m}$ hole. The three different materials Silicon carbide, Silicon nitride, and Indium antimonide are assign to PnC array. It is analyzed that PnC consist of $8\mu\text{m}$ air inclusion employed with silicon carbide give widest bandgap between 2485MHz and 2745MHz in desire frequency ranges. It is also observed that by increasing the air hole inclusion the bandgap also increase.

CHAPTER 1

Introduction

1.1 Overview

This chapter contains detailed introduction of background of the study, problem statement, objectives and significance of the proposed study. It also consist definitions of key terms of the study, advantages and disadvantages.

1.2 Background of Study

A phononic crystals (PnCs) is an artificial wave form structure, which is similar in appearance to a crystal lattice, and is broken in a regular order in the host matrix. Phononic crystals have a basic function which is to show the forbidden limit of frequencies. Phononic crystals with elastic and acoustic properties that change in space on a regular basis. In view of their regularity, they display a whole band gap in which the movement of elastic waves is prohibited in all direction of the space. In addition, the band structure of these systems permits the management and engineering of elastic waves, paving the way for many functions such as signal processing, filtering, negative refraction, and sound separation. The dispersion curve with negative slope is presented in the band structure of phononic crystals, which include negative refractive effect of phononic gaps material that are able to movement of mechanical waves at certain frequency ranges.

At specific set of frequency ranges the flexible waves cannot propagate known as the phononic band gap. Phononic crystals are designed to control, and manipulate the movement of sound waves in a substance. For example, the presence of band gaps may prevent phononic crystals from promoting flexible waves inside a structure. The band gap is a frequency limit that does not allow an audible, guided process or wave movement within the design. Most of the phononic crystals are made from Microelectromechanical-system (MEMS) materials but it can also made from magnetic materials[1].

Many wide-band phononic crystals have been designed, but the PnC is the most often used type. Its unit cell is made up of four-square convex gaps at the corners and a cross-shaped concave gap in the centre. A low frequency band gap can be created by combining convex and concave edges. A one-dimensional holey phononic crystal strip that resembles a convex shape and has several

large band gaps yet a straightforward manufacture is studied. Narrow band gaps with a hard-spatial dimension could exist because of the deformable L-shaped connections with PnC that fix the folding topology. Moreover, a wide range of geometrical parameters can be used to modify the maximum band gap of up to 63% that can be produced [2].

There are few characteristics of phononic crystals, such as the structure of an acoustic band. Phononic has a periodic form which is flexible and sound, giving indication of the constant changes in space. In any direction of the space, they show a complete band gap. The periodicity of phononic crystals plays a role in bandgap and dispersion tuning. Moreover, a phononic crystal is composed of a mixture of materials that allow interactions, holds and propagation of waves to be required for any medium. For certain frequencies the waves cannot propagate in the material referred to bandgap. There is a blockage of all types of mechanical waves and they are distinct from the phononic band vacancy. Phononic crystals control surface waves, sound waves, and flexible waves, among other types of mechanical waves.

At specific frequency there are spaces for sound waves and flexible waves in phononic crystal. The defective dispersion manifests in the band gaps when a phononic crystal defect occurs. Therefore, it is possible to accumulate and direct wave propagation using the design of flaws in the ideal phononic crystal [3].

Between the resonator and the substrate, phononic crystal is reflected back to the resonator, isolating the transmission of elastic and acoustic waves. One of the most popular methods among these technologies for minimising the loss of MEMS resonator anchor points is the use of phononic crystal (PnCs) architectures. One-dimensional (1D) phononic crystals can make the device extremely sensitive to mechanical vibration, but two-dimensional (2D) phononic crystals also provide a high-quality factor [4].

The surface Acoustic Wave propagation in a nanoengineered phononic system consisting of one, two, and three dimensional phonon structures. The band gap is defined in a different place for each of these buildings. Another good step to expand phononic material applications is the creation of two sets of dimensions in a single technology process, but only with an identical material. For our research, we are using nondestructive testing methods.

To determine the SAW dispersion relation, a Brillouin scattering of light has been applied. The finite element technique (FEM) has been used to perform theoretical computations of the predicted dispersion relation. Our study's primary objectives were to ascertain the impact of

pillars and stripes, two different types of nanostructures, on the dispersion relation of surface acoustic waves in a phononic crystal made up of these nanostructures and the type of vibrations that arise at the interface between these two nanostructures[5].

1.3 Types of Phononic Crystals

PCs can be classified into two categories: acoustic phononic crystals (APCs) with a fluid matrix, and elastic phononic crystals (EPCs) with an elastic solid matrix.

1.3.1 Acoustic phononic crystals /metamaterials

The term "metamaterials" refers to a class of synthetic materials whose properties are different from those of ordinary materials yet do not violate objective physical laws. The initial field that influenced the concept of metamaterials was electromagnetics. When theoretical physicist Veselago of the former Soviet Union found that electromagnetic materials have negative permeability and dielectric properties as opposed to conventional materials with positive material parameters, he theoretically proposed electromagnetic metamaterials in 1968. Because of its magnetic permeability and negative dielectric constant, this kind of optical material has a negative refractive index. The outgoing streams and the incident are on the same side of the normal line, not across from it. The wave vector K, the strength of the electric field E, and the intensity of the magnetic field H have a left-handed connection. Left-handed or double negative content is the term used to describe this kind of information. It is necessary to build an analogous optical metamaterial with a structure significantly smaller than the sub-wavelength scale in order to make an audio metamaterial.

Band gaps are defined as specified frequency ranges when the acoustic metamaterial's effective characteristics turn negative (see Figure 1.1 & 1.2). Natural materials have positive material parameters such mass density, Young's modulus, and Poisson's ratio; but, in artificial construction, the effective material parameters can go negative in certain frequency ranges. When mechanical waves travel through this kind of construction, their propagation is impeded by the modulation of the structure, which produces an effect of vibration isolation and sound absorption.

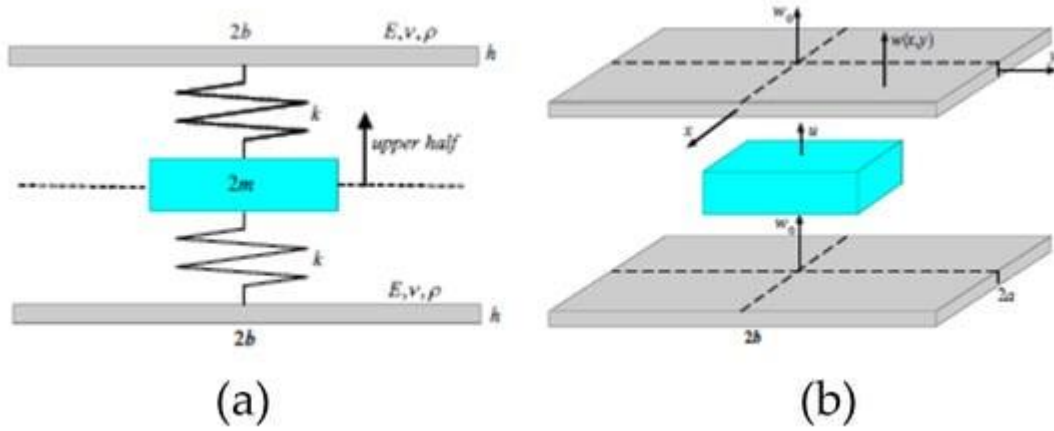


Figure 1.1 An example of a typical acoustic metamaterial plate unit cell (a) front view; (b) perspective view[6].

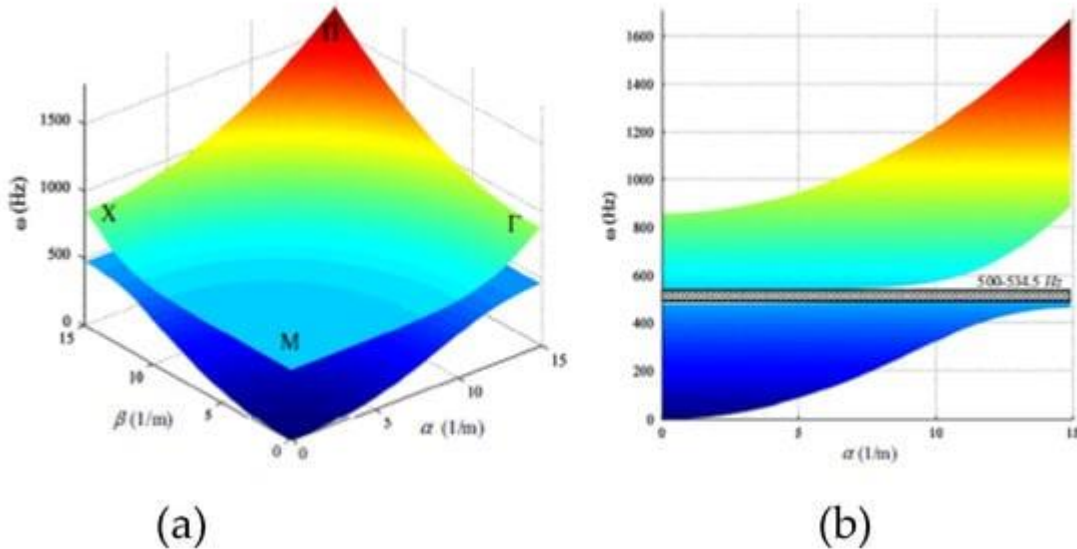


Figure 1.2: The metamaterial above's dispersion surfaces and band gap (a) dispersion surfaces; (b) stopband (gray rectangle) [6].

1.3.2 Elastic phononic crystals / metamaterials

The study involved manipulating the internal architecture of elastic metamaterials including hexagonal unit cells. Higher frequency bands resembling FCC unit cell models exist in addition to pentamode bands. Nevertheless, by disrupting the unit cell's symmetry, band gaps at low frequencies were achieved. Low-frequency band gaps and pentamode bands are of particular interest because of their considerable potential in applications. We examined the impact of the

geometric and structural elements on their band gaps or pentamode bands. Band widths and band gaps of the pentamode bands can be adjusted, and the bands can be converted into different bands by adjusting the parameters. Through the use of finite element analysis tools, materials made up of hexagonal unit cells were simulated in order to confirm the presence of the bands. We checked the transmission of the shear and compressional stresses by applying harmonic boundary loads.

This is how the thesis is organised: Standard primitive cell is covered in Section 2, and subsequent sections will vary it. Modifying the primordial cell in various ways is covered in Section 3. Their differences in internal architecture lead to their classification into four groups. The two specific models with a band gap and a pentamode band are the subjects of the simulations in Section 4. The argument regarding primitive cells is covered in Section 5. Conclusion of the study is given in Section 6[6].

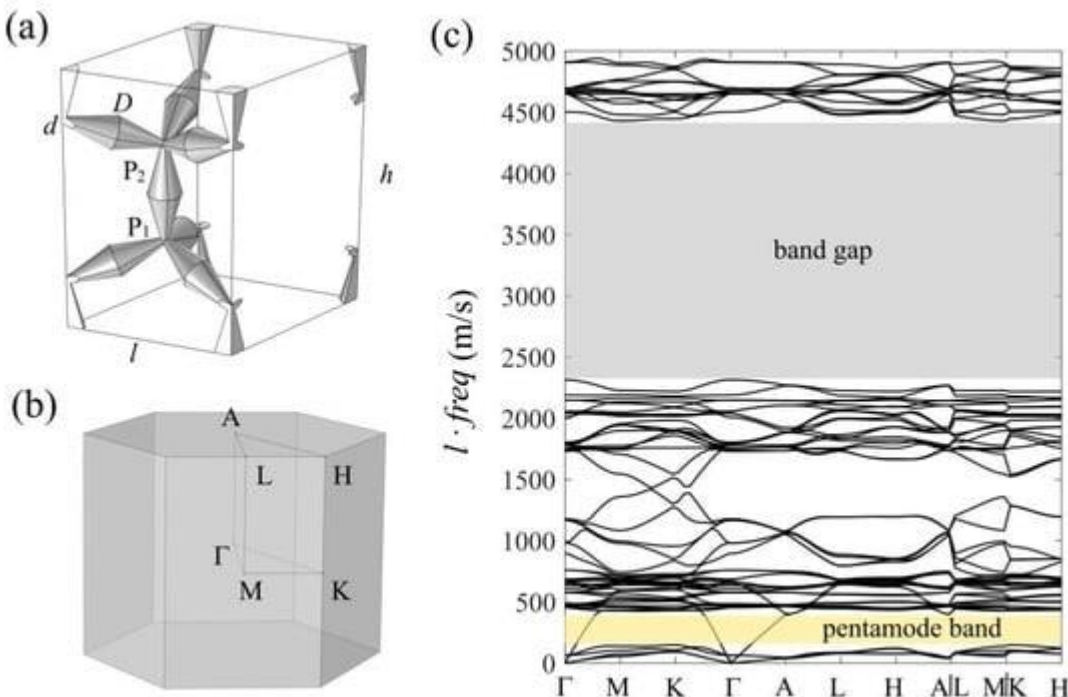


Figure 1.3: Hexagonal unit cells in elastic metamaterials: (a) primitive cell; (b) Brillouin zone; (c) band configurations surrounding the irreducible Brillouin zone's edges [7].

The peculiar physical characteristics of periodic composite materials, also referred to as phononic crystals, have drawn more attention to the propagation of elastic waves in these

materials. Among these characteristics are phononic bandgaps, which specify the frequency range in which elastic wave propagation is not permitted. Many possible uses, including vibration and noise absorption, are made possible by the presence of phononic bandgaps. Bragg scattering and local resonance are the two processes that lead to bandgap creation. The phononic bandgap's corresponding wavelength in Bragg scattering is the same order as the structure's periodicity. Accordingly, phononic bandgaps for the low frequency range can only be obtained with a large lattice constant, which restricts application possibilities. Two orders of magnitude smaller wavelength is required to produce local resonance than the Bragg bandgap. Dependent less on the periodicity and symmetry of the structure, a locally resonant bandgap is linked to the resonance frequency associated with scattering units. Consequently, it circumvents Bragg bandgap limitations and allows bandgaps appropriate for lower frequencies [7].

1.4 Phononic crystals resonator

In actuality, phononic crystals are acoustic waves with periodic formations similar to the crystalline structure of electrons; acoustic waves are also occasionally referred to as elastic waves. Artificial materials structured in a highly ordered microscopic structure of a variety of particles are called phononic crystals. Over the last 20 years, phononic crystals, or PnCs, have drawn the interest of scientists. Particularly in the area of information and communication technologies, phononic crystals have a wide range of possible uses. Phononic crystals have the ability to influence the propagation of waves. Phononics is a rapidly developing field.

The field of phononic crystals has made significant strides in recent years. Phononic crystals (PnCs) MEMS resonators are a subject of great interest to scientists and engineers. The PnCs play an important role in the development of micro- These days, phononic crystal research has made significant strides. Engineers and scientists are focussing on deep and nanofields. PnCs enabled tether arrangements to separate the energy transfer from the resonator body into the substrate. The design of apparatus such as waveguides and cavities to regulate the propagation of sound waves inside the band is made possible by a perfect PnC. PnCs have the ability to function as coupling elements amongst resonators. Furthermore, the integration of PnCs with n-type doped silicon within nanostructures presents a viable option for thermoelectric uses [8].

1.5 Phononic Crystals and Thermal Effect

Complete phononic bandgap formation and partial halting of thermal phonon transport

are possible with a well-designed PnC. The bandgap's low frequency and too-limited frequency range for the wide thermal phonon spectrum, however, limit the effect. All forms of mechanical waves are virtually blocked within the phononic band gaps. The fluctuation in the mechanical characteristics of the materials that make up the PnC structure is actually responsible for the development of the phononic band gaps. The interface between each of the two materials can so produce Bragg interference. It leads to the formation of transmission bands and phononic band gaps [9].

1.6 Dynamics of Phononic Structures and Materials

The dynamics of phononic structures and material involve studying how mechanical vibrations propagate through materials, affecting their mechanical, thermal, and acoustic properties. This field explores phenomena like phonon dispersion, wave propagation, phononic band gaps, and phonon-phonon interactions to understand and manipulate material behavior for various applications, including acoustic insulation, energy harvesting, and phononic devices [10].

1.7 Band gap and phononic crystal

Phononic band gap materials can prevent mechanical waves from travelling in specific frequency ranges. The band gaps result from the combination of different phases with distinct properties within a single material.

Various mesoscopic phononic materials have the capacity to display frequency bands that prohibit transmission, known as band gaps. These band gaps originate from three distinct mechanisms: Effects of Bragg, hybridisation, and feeble elastic coupling. Due to the destructive interference of waves scattered from inclusions, Bragg gaps are a frequent feature of phononic crystals. These spaces can either solely follow certain directions (stop bands) or restrict wave propagation in particular frequency ranges in all directions (band gaps). Most remarkably, band gaps of various origins may also be seen in mesoscopic structures. For example, band gaps resulting from hybridisation gaps can be linked to the coupling between the propagating mode of the embedding medium and the scattering resonances of individual inclusions [11].

1.8 Tunable Topological Phononic Crystals

The astonishing one-way propagation edge states in photonic and phononic crystals, which are supported by topologically nontrivial band gaps, are inspired by topological insulators, which were originally identified in electronic systems. By violating the time-reversal symmetry, one can create such band gaps by lifting the degeneracy connected to Dirac cones at the Brillouin zone's corners. The creation of a phononic crystal with a Dirac-like cone in the centre of the Brillouin zone, which breaks time-reversal symmetry and modifies the unit cell's geometric size to produce a topological transition that is confirmed by edge-mode analysis and the calculation of the Chern number. A comprehensive model built on the tight binding to reveal the underlying physical processes of the topological change. The model and numerical simulations both demonstrate that the band gap's structure is changeable by altering the geometric size as well as the velocity field; this tunability may significantly enrich the creation and application of topological insulators for sound[12].

1.9 Surface Acoustic Waves in Phononic Crystals

On millimeter-scale periodic structures with band gaps occurring at frequencies of a few megahertz or less, SAW in two-dimensional phase transitions was carried out. There were additional demonstrations of surface modes and localisation events in linear and point defects. applications in radio frequency (RF) communications or MEMS devices at the micrometre scale, which did not begin to take shape until the mid-1900s. Surface acoustic wave propagation via pulsed ultrashort optical stimulation and detection is photographed in two dimensions in real time at frequencies up to 1 GHz on a microscopic two-dimensional phononic crystal composed of a square lattice of holes. Surface waves propagating parallel to the phononic crystal axes exhibit the opening of stop bands at the zone boundaries, as indicated by the acoustic dispersion relation derived from spatiotemporal Fourier maps [13].

1.10 Problem Statement

Phononic crystals rotate around the structure, and purpose of materials which show phononic band gaps, which as same analogy as electronic band gaps in semiconductors. Such band gaps, similar to those in semiconductors where certain energy levels of electrons are blocked by the electronic bands, prevent some frequencies from being transmitted through a material. Phononic crystals are structured materials that regulate the mechanical waves' ability to propagate, like sound or vibrations. The phononic crystal is used to transmit and disperse mechanical waves in the desired frequency range. It includes the different aspects of design, construction, material selection and wave propagation modeling.

1.11 Aims and Objectives

These are materials that have a periodic structure and are designed to control the propagation of sound waves through them. The main purpose of this research is

- i. To find the suitable material for proposed structure
- ii. To manipulate the propagation of elastic waves in structural design
- iii. To enable the tuning of dispersion and routing of surface acoustic waves

1.12 Significance & Scope of Study

Those are the type of metamaterials that show the ability of different acoustic properties because the acoustic wave's propagation is mostly impossible in chemically assumed substances. Phononic crystals are regularly flexible compound that has large application possibility in controlling and managing flexible waves. The reason is the essence of phononic band gaps. The band design of phononic crystals show dispersion curves that have negative bending, making phenomenon in which propagation of waves is bent towards the negative. Phononic crystals reduce frequency noise effectively, because their particular resonant system works like a spatial frequency filter.

1.13 Definitions Of Key Terms Of The Study

1.13.1 Phononic Crystal

The control over the passage of sound waves by a periodic structure is known as phononic crystal, and it works similarly to the control over electromagnetic wave propagation by a regular crystal lattice. It consists of a regular array of materials with alternating acoustic properties, such as density or elastic modulus, which creates a bandgap where certain frequencies of acoustic waves cannot move up through the structure. Phononic crystals have applications in sound insulation, acoustic filters, and even in designing materials with specific acoustic properties[14].

1.13.2 Microelectromechanical system

Microelectromechanical systems (MEMS) in phononic crystals refer to the integration of miniature mechanical structures or devices within the phononic crystal framework. These MEMS devices can be designed to interact with acoustic or mechanical waves in specific ways, taking advantage of the phononic crystal's properties for various applications such as sensing, signal processing, or actuation. By combining MEMS technology with phononic crystals, engineers can create compact, efficient systems with precise control over acoustic waves, enabling advancements in fields like telecommunications, medical imaging, and structural monitoring[15].

1.13.3 Dispersion tunning

Dispersion tuning in phononic crystals refers to the capacity to control the dispersion relation, which describes how the frequency of a wave depends on its wavevector (or momentum). By adjusting the parameters of the phononic crystal, such as the lattice spacing or material properties, engineers can manipulate the dispersion relation to tailor the behavior of acoustic or mechanical waves within the material. This tuning capability allows for the creation of band gaps, waveguides, and other desired acoustic properties, enabling precise control over wave propagation for various applications in signal processing, sensing, and wave manipulation[16].

1.13.4 MEMS Resonator

A MEMS (Microelectromechanical Systems) resonator is a tiny mechanical device that vibrates at a specific frequency when stimulated by an external signal. These resonators are fabricated using microfabrication techniques and can be integrated into electronic circuits for various applications, including frequency reference, timing, filtering, and sensing. MEMS resonators provide benefits such compact size, low power consumption, good frequency stability, and compatibility with methods used in semiconductor manufacture. They are commonly used in devices such as oscillators, gyroscopes, accelerometers, and filters[17].

1.13.5 Surface acoustic wave

A surface acoustic wave (SAW) is a kind of mechanical wave that passes over a material's surface, usually a quartz piezoelectric substrate. These waves are a specific form of acoustic waves with particle motion confined to the surface, and they can be generated and detected by transducers placed on the material's surface[18].

1.13.6 Electromagnetic material

An electromagnetic material refers to a material that exhibits specific properties related to the manipulation and control of electromagnetic waves. While phononic crystals primarily deal with the control of acoustic or mechanical waves, some designs incorporate electromagnetic properties as well[19].

1.13.7 Mechanical waves

Mechanical waves in a phononic crystal refer to waves that propagate through the material's structure as vibrations or oscillations in the mechanical elements of the crystal. These waves can include acoustic waves (sound waves) or other types of mechanical vibrations, such as elastic waves in solids[20].

1.14 Advantages of phononic crystal

Phononic crystals are a type of metamaterial, and advances in metamaterials have influenced the development of phononic crystals. Negative refraction, superlensing, and cloaking effects have been demonstrated using phononic crystals, leading to potential applications in

acoustic and thermal management. Phononic crystals are being used to design advanced noise canceling materials and vibration isolators. These materials can be applied in various industries, including automotive, aerospace, and construction, to enhance soundproofing and reduce unwanted vibrations.

Phononic crystals can control the flow of heat at nanoscale, making them useful in thermoelectric devices and thermal insulation. By manipulating phonon transport, these materials can improve the efficiency of heat engines and refrigeration systems. The creation of extremely sensitive sensors for detecting sound waves and mechanical vibrations has made use of phononic crystals. They also have potential applications in signal processing, such as in the design of acoustic filters and waveguides.

1.15 Disadvantages of phononic crystal

In the bulk of previously described phononic crystal devices, large structures confined to frequencies below 1MHz have been created by manually constructing scattering inclusions in a viscoelastic media, mainly air, water, or epoxy.

It has been possible to scale devices and phononic crystals to VHF frequencies (30–300 MHz) and higher recently by using microfabrication and micromachining processes. The current state of research on micro-phononic crystals is reviewed in this thesis, along with design strategies, material analysis, microfabrication procedures, description techniques, and documented apparatus configurations. The potential uses of low-loss solid-state micro-phononic crystal devices in radio frequency transmission and audio visual for nondestructive testing and medical ultrasonography are emphasised.

CHAPTER 2

Literature Review

A phononic crystal is composed in one, two, and three-dimensional lattices of a regular order of acoustic scattering. These scattering centers shows the various acoustic properties[21]. The wave propagation in phononic crystal indicates the state of acoustic band gap development and its role as a resonance. In order to be elastic metamaterials, phonon systems potential is exploited[22].

The category of phononic crystals and the phenomena of phononic crystals with two, and three-dimension crystal structure in locally beaten materials are based on physical characteristics. Phononic crystals micro electromechanical system resonators that have various transduction plan such as electrostatically , piezo resistively , piezo electrically changed micro electromechanical system resonators are explained[23]. A method that is designed to detect, surface acoustic waves up to 50 GHZ in hyper sound frequencies used for sensing and Nano metrology applications with high potential can be developed using Nano-structure surface phononic crystal[24].

At Nano scale, phononic crystal is able to control temperature transport and coherent phonon in a single dimension. By regulating phonon properties at the Nano level, a one-dimension phononic crystal has become an essential optoelectronic component for electronic devices[25]. An unusual core structured is presented to allow the bending bands to form a gap that do not affect the structural deformation strength of design of Phononic crystal. Two researchers Ampatzidis, and Chronopoulos examined the phononic crystal of low frequency stop bands with two different core schemes. The inertial nature of the structure from Meta material which provided referenced design in low frequency and light materials, vibration isolation device[26].

It is important for many applications to control thermal transport at the Nano level. The three-dimensional structure of phononic crystals may also control thermal conductance. In the same way, two photons lithography is applied with heating in order to

build structures for 3D phononic crystals within a hypersonic range of frequencies. The results showed that conductance can be enhanced with changing the structure of phononic crystal. This technique is based on 3 dimension structure design, which is so complicated[27].

Yan and his coworkers presented the phononic crystal to determine the wave propagation properties of two-dimensional useful classification regular grid design by the count of the flexible oscillator. The wave dissipation relation of the regular grid design with local resonators are affected by the spectral component process. The effectiveness of the band gap calculation way is proved by the transfer of vibrations of the fixed length grid structure that depend on the spectral element method and fixed component method. The effects are analyzed of the structural and material parameters on in-plane mode wave propagation properties that can be applied to the vibration. Because of its intentionally created band gap characteristics, phononic crystal structures have the ability to draw greater attention and attention in the fields of vibration control and loud acoustics. Phononic crystal with H-shaped radial structure is offer to stop the anchor deficiency of a Lamb wave resonator, with an ultra-wide band characteristic and also has high ultra-frequency. For holding the anchor deficiency of the Lamb wave resonator, radial phononic structure is more reliable.

The use of complicated valued eigen wave vectors or eigen frequencies that represent space-based elastic wave attenuation is a natural consequence of the study of material loss in phononic crystals. If elastic losses in viscoelastic substances are proportionate to frequency, phononic band configurations with complex eigen frequencies but real wave vectors shall be obtained[28].

An unbaked lattice model, which takes into account the structural properties of a crystal that does not contain material, can be used to analyse the process through which anisotropic phonon crystals produce Bragg band gaps. This approach makes it possible to learn how lattice geometry influences the propagation of sound waves, leading to bands being closed. The anisotropic nature of the band gap introduces a directional dependence, which influences wave propagation from one crystal orientation to another. The band

structure's numerical computations verify that the junctions anticipated by the matrix's empty lattice model have avoided crossings and, as a result, Bragg band gaps emerge around them[29].

Scalar waves have an amplitude and a phase, but they don't polarize. The band structure describes the dispersion relation, which relates the wavevector (\mathbf{k}) to the frequency (ω) of allowed wave solutions in the crystal. In view of the interactions between neighbouring cells, this process usually consists in discretising a crystal unit cell into individual cells so that it can solve its wave equation. In order to calculate the crystal's overall response accurately, GMT uses multipole expansions for representing fields and currents in each cell. A band arrangement can be calculated in the region of Brillouin, using a variation of wavevectors that correspond with frequencies allowed and their corresponding waves. The structure of the band reveals information about gaps in frequencies where propagation is not allowed, as well as regarding the nature of permitted modes within a crystal[30].

A phenomenon in which elastic waves, such as sound or seismic waves, interact with a periodic arrangement of spherical objects, leading to scattering and interference, is flexible wave spreading by regular design of spherical mass. Theoretically, these phenomena is frequently examined using techniques like the Mie or multiple scattering theory, which take into consideration the interactions between the spheres and the incident wave. For experimental purposes, specially designed structures with regularly spaced spherical objects may be examined using techniques such as acoustic or seismic measurements. These experiments help to confirm the theories and gain insight into the behavior of elasticity waves in a complex media[31].

Depending on their size, shape, material and location, sculptures can be able to mitigate noise. Sound waves can be absorbed by sculptures that have irregular surfaces or impermeable materials, which reduce noise levels around them. In addition, sculptures strategically placed in open space may contribute to the redirection of sounds and mitigate their effects on neighbouring areas. Sculptures can absorb or diffuse sound waves, contributing to the attenuation of noise. Materials and shapes play a role—porous surfaces absorb sound, while irregular shapes scatter it. Noise pollution can be mitigated by the

installation of such sculptures in public spaces[32].

Sound waves propagating through a medium with varying density are referred to as the periodic density fluctuations in fluids' acoustic band structure. The phenomenon is often associated to phononic crystals. These materials have a periodic arrangement of acoustic properties, which influence the dispersion of sound waves. The sound band structure of these systems describe the frequency range bands that are permitted to be used for sounds. Band gaps, where certain frequencies cannot be transmitted through the medium, are caused by periodic density variations. For engineering materials with special acoustical properties, such as for the development of sound filters, it is essential to understand these band structure[33].

In areas such as insulation, vibration control and the development of novel sensors, phonon crystals are an exciting area that has promise for applications. Improvements in the design of phonon crystals with special band gaps, exploring new materials for enhanced performance and investigating dynamics tunability have been reported recently. Potentials include the integration of phonon crystals in real devices, improving their efficiency and discovering new applications such as telecommunications and medical imaging[34].

In various areas, such as acoustics, optics and materials science, high frequencies phonon crystals have shown encouraging advances. Research has been carried out recently to optimise their design for control and modulation of sound waves at higher frequency, which could lead to future applications in sensing, imaging or communication technology.

Further understanding of their essential characteristics and exploring new possibilities for implementing them in practice are the focus of continued efforts. Phonons can be considered as the quantization of waves which disperse in the medium with a velocity of sounds which depends on the elastic properties (stiffness and mass) of materials. Not only in science, but also in everyday life and industry, the importance of phonon is recognised. The phonon's frequency is audible in a wide range between few Hz and dozens of THz, where only the narrow band from 20 Hz to 20 kHz can be heard. In a variety of applications, the inaudible phonon is important because of its frequency. Infrasound, for example, has a high transmissivity at frequencies below the limit of man audibility, which

enables it to overcome obstacles with little dissipation, so it is used as an important detection technique in the study of seismology. At higher frequencies above the upper audible limit, such as ultrasound (from 20 kHz - 1 GHz) is in imaging and non-destructive testing tools , hypersound (from 1 GHz to 1 THz) is utilized in the signal processing and acousto-optics devices, and the higher frequency (>1 THz) range is responsible for thermal transport and thermal management. To that end, the modulation in the same way as those remarkable results for manipulating electrons and photons[35].

Tunable and active phononic crystals and metamaterials" could highlight the importance of these materials in controlling sound waves and vibrations, their applications in various fields such as acoustics, engineering, and material science, and recent advancements in making them dynamically adjustable and responsive. Key concepts such as bandgap engineering, wave control and the potential for new device design and function could be mentioned. Anomaly wave propagation behaviour, tunable mechanical configuration, materials with multifield coupling, and tunable wave manipulation based on distinct regulation methods are some of the recent advancements in tunable and active PC and MMs. The tunable and active phononic crystals (PCs) have significant potential in various fields due to their ability to exhibit abnormal properties through artificial design of unit cells[36].

L-shape triple defects in a phononic crystal could enhance broadband piezoelectric energy harvesting by creating multiple resonance modes that can capture energy across a wider frequency range. The efficiency of energy conversion from mechanical vibrations to electrical energy is increased by this design innovation. The inclusion in the PnC of a proposed design concept called Lshape triple defects can overcome the limitations on single and double defect-in-corporated systems. The isolated single defect at the top vertex of the letter 'L' compensates for the limitations of double-defect-incorporated systems, whereas the double defects at the bottom vertices compensate for the limitations of the single-defect-incorporated systems. In this way, an effective limitation of the elasticwave energy on Broadband frequencies and a more efficient harvesting of it can be achieved as well as increased application of Single and Double Downdrafts[37].

In fact, for the detection and harvesting of elasticity wave energy in a broad spectrum, phononic crystals with various defects can actually be useful. It can create a crystal that responds to any frequency range, and optimize energy harvesting by strategically adding defects of various properties such as size, shape or structure.

An innovative idea for PnC design that looks at the many arrangements of the twofold flaws of energy localisation and harvesting in broadband elastic waves. For instance, when a pillar is absent, a square pillar-type unit cell is taken into consideration, and a construction with a single piezoelectric patch bonded to the host square lattice is deemed defective. Each flaw is a single independent defect if the two introduced faults in the PnC are far enough apart to allow decoupling behaviours to be implemented. In this case, the differences in the same stiffness and inertia of the defects contribute to the individual manipulation of the defect bands corresponding to each defect, by distinguishing the geometric dimensions of the two piezoelectric patches. Defects with varying equivalent mass and stiffness help to produce discrete yet independent bands of defect if the piezoelectric patches have diverse geometric dimensions. As a result, we are able to harvest patches along with localise the elasticity wave energy transfer in Broadband by correctly spacing Independent Frequency Response Function's for performance of PEH Welldesigned frequencies.

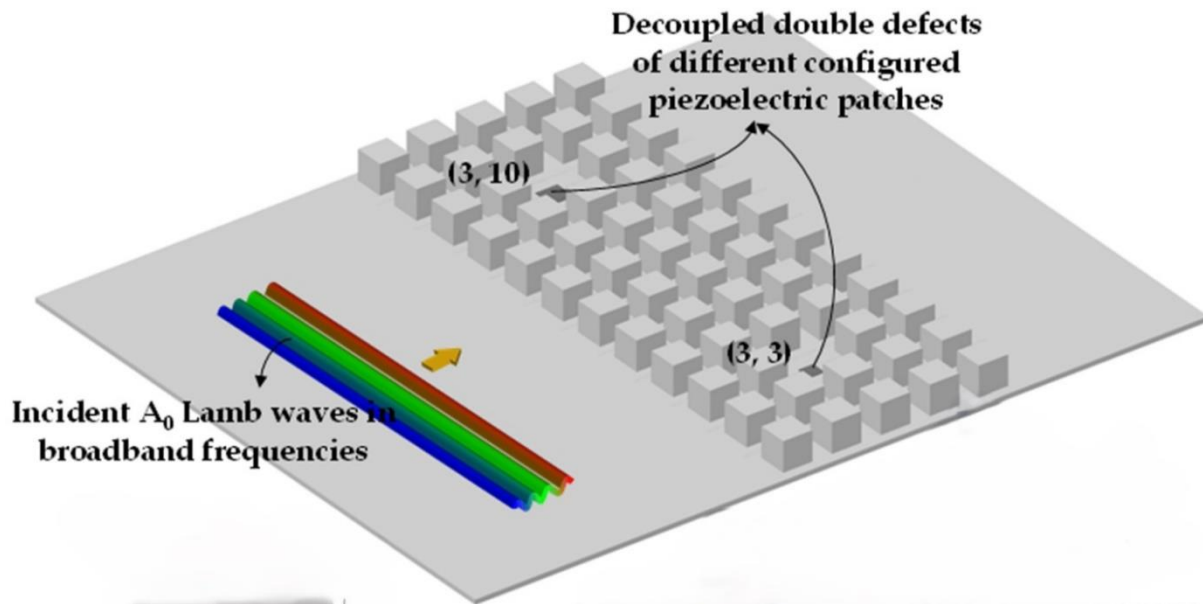


Figure 2.1: An illustration showing the decoupled double defects of a two-dimensional square-pillar-type phononic crystal (PnC).

From figure 2.1 show that the schematic representation of a two-dimensional square-

pillar-type phononic crystal (PnC) with decoupled double defects that has been equipped with variously arranged piezoelectric patches for the purpose of harvesting and localising broadband energy in relation to right-going incident A0 Lamb waves.

The unit cell shall consist of an aluminum square lattice, which shall be affixed to the top surface by an aluminum square pillar; the square pillar shall be placed at the center of the lattice. The PnC will be a 5*12 configuration of the unit cells. Simultaneously, two square pillars at positions (3, 3) and (3, 10) are eliminated, and square piezoelectric patches of PZT-5H (lead zirconate titanate, $Pb(ZrxTi1-x)O_3$) with distinct geometric dimensions are adhered to the upper surface of every aluminium lattice. These patches are dark-gray in colour. Each piezoelectric patch is coupled to an external electrical resistance and an alternating current to direct current (AC-DC) converter [38].

Two GaAs/AlAs superlattices (8 nm/8 nm and 5.4 nm/5.4 nm) at room temperature were found to exhibit a quantum coherent connection between a zone centre phonon and two acoustic phonons. When the driving phonon mode near the centre of the first Brillouin zone and the two target acoustic phonon modes exchange coherent energy, a multi-cycle oscillation feature is observed in the time-resolved phonon amplitudes of both samples using degenerate coherent phonon spectroscopy. The investigation of the interaction between phonons in a semiconductor structure material, which provides insight into quantum coherence phenomena, could be highlighted with regard to Phonon phonon Quantum Coherence couplings at GaAs superlattice. The study is likely to examine how the periodic arrangement of atoms in a superlattice has an effect on phonon dynamics and coherence, which could lead to advances in phononic devices or quantum information processing[39].

To improve the motional impedance (R_x) and mechanical quality factor (Q), acoustic mode confinement is accomplished through the use of specially designed mechanically coupled acoustic cavities, also referred to as acoustic Bragg Grating Coupler structures. This allows the vibration energy within the resonators to be spatially localised. This improvement in the mechanical response has been demonstrated by numerical simulations utilising several proprietary resonator technologies involving dielectric transduction. The

connection of the cavities serves as the basis for the resonator's design, which are the material areas that are integer multiples of the length of the acoustic wavelength. Acoustic mode confinement using coupled cavity structures in UHF unreleased MEMS resonators refers to a technique used to control and confine acoustic waves within micro electromechanical systems (MEMS) resonators operating in the ultra-high frequency (UHF) range[40].

A photonics structure composed of a number of optic resonators, such as ring resonators or micro disks, coupled to one another is referred to as the Coupled Optical Resonators waveguide CROW. These resonators are typically connected with waveguides, which allow light to flow through them. CROWs find application in various photonic fields, including delay lines, sensors, and filters. An innovative kind of optical waveguide made up of a series of connected high-Q resonators. In contrast to other kinds of optical waveguides, the coupled-resonator optical waveguide (CROW) achieves wave guiding by means of weak coupling between high- Q optical cavities that are otherwise localised[41].

Two dimensional dynamic directional amplification of phononic metamaterials involves the design of materials that can amplify or control the propagation of mechanical waves, such as sound, in specific directions. At wavelengths well beneath the wavelength range to which bandgaps are generated as a result of space periodicity, patterns of phonons with unit cells that exhibit Dispersion Bragg and local resonance have special wave propagation characteristics. However, both mechanisms suggest that the design of systems with wide bandgaps at low frequencies may be subject to some constraints. In order to achieve the proposed results, it is possible to impose Kinematic limitations on the structure's level of flexibility, DDA, DoF, growing moments of inertia and reducing the intended motion's direction. Bloch's theory is used to analyse the 2D lattice, and the similar dispersion relations are obtained. A 2D lattice analysis is carried out using Blochian theory, and the associated dispersion relations are obtained. Significant enhancements and benefits in comparison to a standard phononic structure, such as wider bandgaps and greater dampening ratios can be seen from the numeric results of an illustrative case study. The concept's use in prospective applications, such as mechanical filters, vibration and sound isolators, and acoustic waveguides, is finally indicated by a

conceptual design.

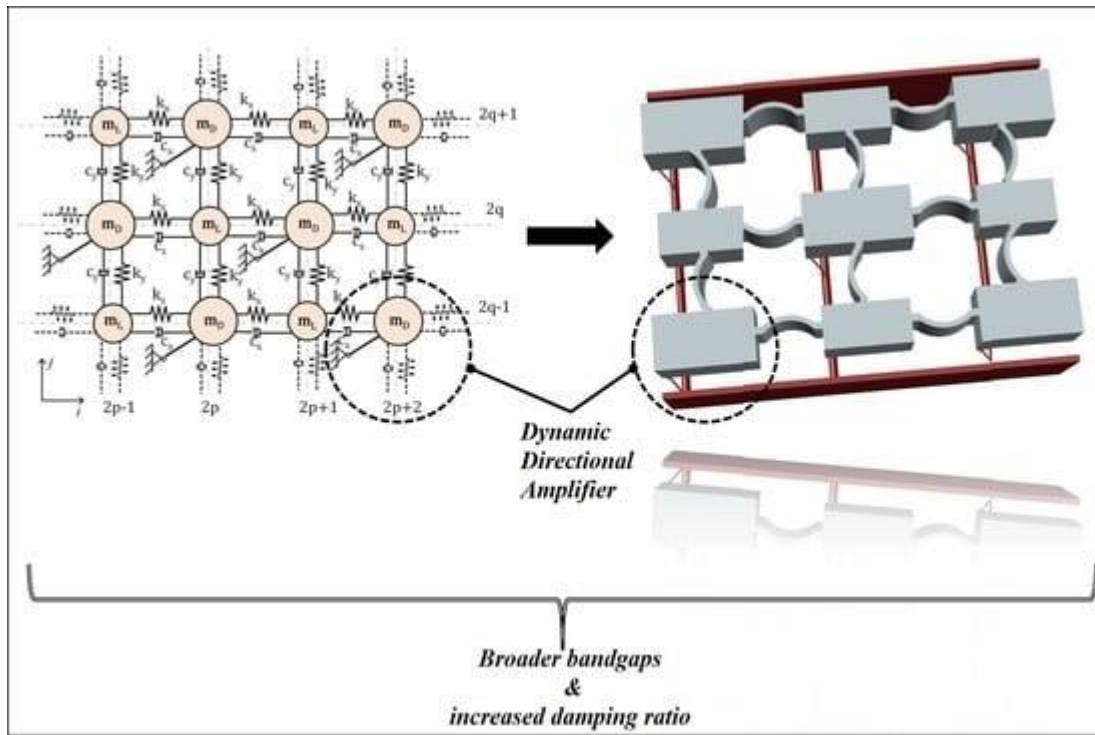


Figure 2.2: Shows the graphical representation of dynamic directional amplifier(DDA).

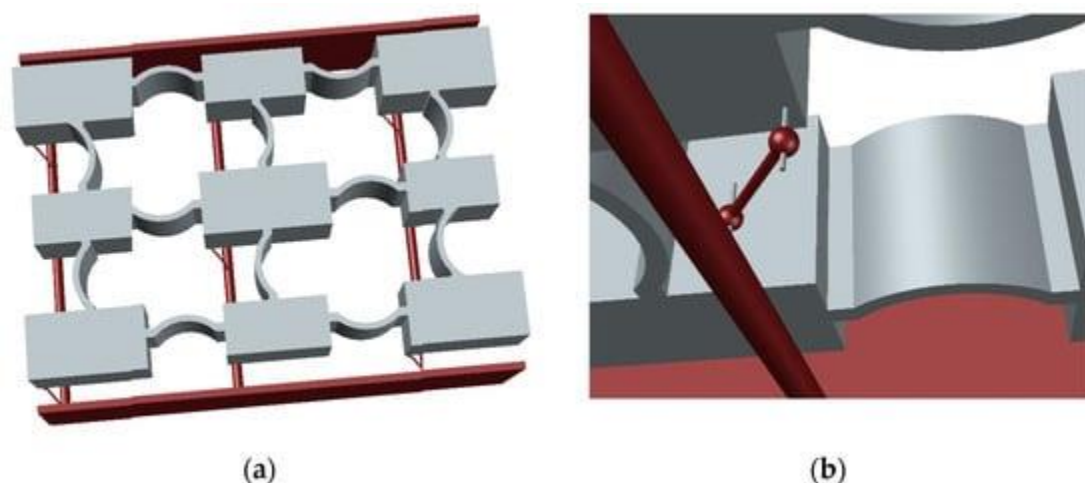


Figure 2.3:Proposal of conceptual metastructure design (a) view of 3 dimension(b) dynamic directional amplifier (DDA) components.

Figure 2.3 shows the suggested metastructure's basic design, which calls for a single unit

cell for simplicity, but allows for the easy construction of bigger lattices through the unit cell's spatial repetition. The massspring lattice, supported by a red colored metal frame, is expected to be a compliant 3D printed part. The frame's function is to make room for the DDA mechanisms at the designated spots, which give the pinned connections overhangs [42].

In a one-dimensional (1D) array of compliant axial to rotary motion conversion systems, phononic band gaps are studied. The unit cell consists of two rings that are joined by bending in cross directions, giving the rings exceptional bending stiffness and minimal torsionality. By means of parallel spiral flexures, the axial stiffness between the top rings is low, and the bending stiffness is high, the uppermost ring of each unit cell is connected to its consequent upper ring.

The efficient inertia of the unit cell mechanism is increased in order to produce a low frequency band gap. The 1D array of this chiral unit cell has been shown to generate a stop band that is limited by two different types of unit cell modes. The phononic band structure and the system's frequency response properties are derived through the use of analytical and finite element models. For the purpose of creating wider band gaps at lower frequencies, parametric studies shall be performed. The unit cell and periodic structure prototypes are created using 3D printing and laser cutting. In order to verify the results, the experimental data is compared with the findings of the analytical and computational frequency response tests [43].

The study focusses on body centred cubic (BCC) and face centred cubic (FCC) lattices with and without inertial amplification techniques that are infinite and finite. To comprehend their impact on the phonon gap (stop band) limits, these three lattice dimensions must be represented using parametrically distinct mass and spring elements. A wide low frequency band gap is produced when one of the infinite periodic lattices use inertial amplification techniques. In addition, the application of few unit cells in order to achieve narrow and deep phonon gaps is needed for an infinite set of regular lattices. For infinite periodic lattices, there could be a band gap. by changing the ratio of mass in their individual cells at different frequency ranges. For most mass ratios, In both BCC and FCC

lattices, the band gap can form, but only within a certain range of mass ratios [44].

As damping is a natural property of materials, its presence in a structural arrangement can have a significant impact on how the structure responds. While dissipation is not wanted in some applications (such energy harvesting), there are many ways to maximise it, such as noise absorption, shock resistance, and vibration suppression. From a design standpoint, rigidity, or mechanical load-bearing capability, is typically sacrificed in favour of an increase in the intensity of damping in the materials used in these latter applications. For instance, elastomeric materials are less rigid but more resilient than metallic ones[45].

Periodic beam-lattices metamaterials with inertial viscoelastic resonators exhibit acoustic characteristics related to elastic, thin ligaments. A basic model comprising a continuous beamlattice made up of kinetic resonators has been built in order to evaluate the impact of the dynamic properties of kinetic resonators and the factors that constitute their vibration on noise activity. The beam lattice is composed of a series of hefty, hard rings spaced obligingly apart by massless, elastic ligaments. An interior resonator composed of a stiff disc in a viscoelastic annulus that is soft completes the lattice. A distinct lagrangian model, described by two relaxation functions, has been constructed that takes into account the elasticity of ligaments connecting lattices and their inertia. This model characterises the soft viscoelastic annulus. Under the simplification assumption of linearised viscoelasticity, an equation of motion is constructed in the Laplace space. It is the basis for the Christoffel equation, which yields the complicated Floquet-Bloch spectrum. The band structure of the lattice without resonators is defined by two acoustical branches and one optical branch. Two acoustical branches and four optical branches are depicted using a band structure typical of propagative waves with or without spatial modulation to account for the existence of inertial resonators [46].

In order to explain the characteristics of wave propagation of a layered lattice structure consisting of a square-shaped periodic sheet topology with antitetrachiral topology, An analytical model of a linear dynamic has been created. By introducing local resonators in the microscopic structure, which are composed of a periodic arrangement of stiff rings and elastic ligaments, an inertial material has been produced. The band structure of the

substance, before marked by a significant spectral density, has been significantly modified as a result of the increased model dimension. Powerful linear relationships between the dispersion curves can be observed as a result of the coupling of an elastic ring resonator. The anti-tetrachiral meta-materials have been observed to provide the largest band gap amplitudes from a physical perspective when they meet two requirements: firstly, they must have a strong ring-to-ligament compositeness of the cell microstructure (maximum admissible ring radius); and secondly, they must have a few large and heavy resonators (maximum admissible resonator inertia) that are weakly coupled with their hosting rings (minimum elastic resonator stiffness). The metamaterial's performance is affected by more than two identical resonators, On the other hand, it is possible to simultaneously achieve a full amplitude in the lowest frequency range by placing two resonators at opposite ends [47].

In a wrinkled soft bilayer system, the defect mode can be changed, potentially making it suitable as a soft photonic crystal. The combined system's band gap being examined relies on the stress pattern caused by wrinkling and is not affected by the degree of compression within the specified range of loading. The faulty mode's frequency seems to change with E. This intriguing observation allows us to adjust the spatial reach of the fault mechanism by just manipulating the applied compressive strain. This research offers fresh perspectives on the adjustability of the fault mechanism in soft metamaterials. The system's defect mode profile can be adjusted without altering the defect itself. Additionally, our approach to incorporating the faulty mode into a composite with soft layers is uncomplicated and direct, making it suitable for various purpose such as the creation of advanced soft metamaterials and related devices[48]. Patterned surfaces are frequently used to manipulate materials. The ability to create and replicate intricate features is crucial for meeting the needs of functional surfaces. Creating wrinkles through the buckling of a rigid film on a flexible surface is a cost-effective, simple, and dependable way to produce a patterned surface. The wrinkling technique has been utilized in numerous fields such as photovoltaics, microfluidics, adhesion, and anti-fouling systems[49].

For phononic purposes, periodic patterning regulates vibrations, which in turn controls the transport of heat and sound into matter. Vibrational modes with minimal dissipation

are realised by bandgaps developing in such phononic crystals (PnCs), opening up possibilities towards advanced sensors, efficient waveguides, and mechanical qubits. Here, we're combining phononics with two dimensional materials and exploring the adjustment of PnCs by applying mechanical pressure. To that end, monolayer graphene is used to manufacture the smallest possible PnC and simulate its vibrational properties. A band gap has been identified within the megahertz regime where a small effective mass of $0.72 \text{ g} = 0.002 \text{ mphysical}$ is detected to localize an defect mode. We use graphene's flexibility to simulate the mechanical tuning of a finite volume PnC. We have observed a 350% increase in the frequency of the entire phononic system under electrostatic pressure up to 30 kPa. Meanwhile, the defect mode stays localised and inside the bandgap, indicating a high-grade mechanical system that is dynamically controllable.

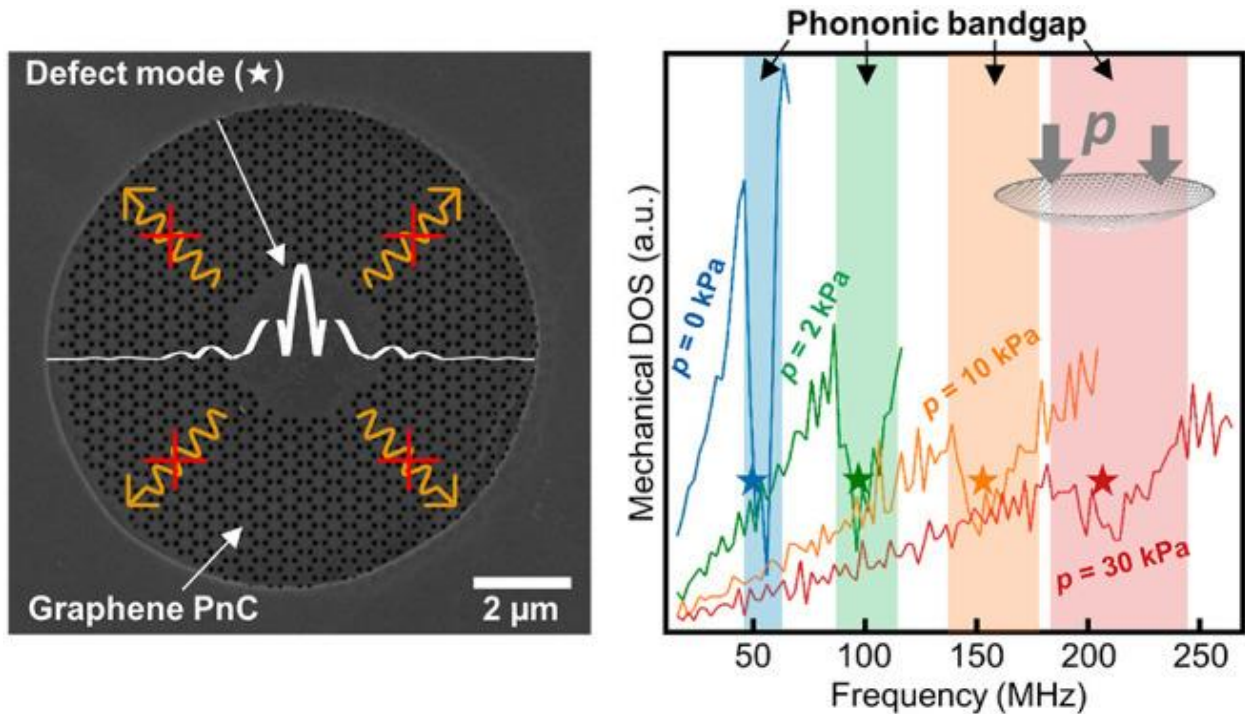
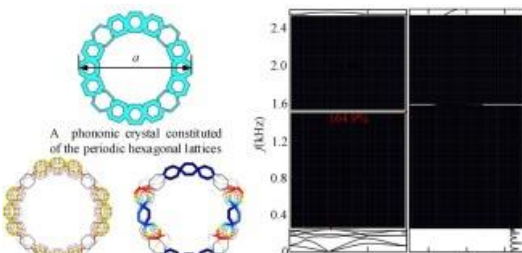
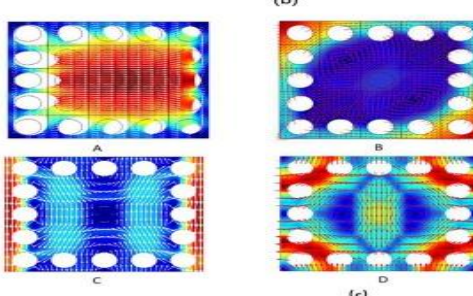


Figure 2.4:(a)Mechanically tunable graphene structure (b) states' density determined using the finite model in relation to the pressure exerted on the hanging PnC [48].

Investigating the behavior of acoustic waves in a two-dimensional composite medium made up of a square array of parallel copper cylinders in air involves both theoretical and experimental approaches. The band structure is determined using the plane wave expansion (PWE) method, applying the condition of elastic rigidity to the solid

inclusions. The results obtained from the PWE method are then compared to the transmission coefficients calculated using the finite difference time domain (FDTD) method for composite samples of finite thickness. In the low frequency range, the band structure calculations align with the FDTD results, affirming that assuming the inclusion to be infinitely rigid maintains the validity of the PWE results in this frequency range. These calculations indicate that this composite material has a significant absolute forbidden band within the audible frequency range. The FDTD spectra also show that hollow and filled cylinders result in very comparable sound transmission, hinting at the potential for creating lightweight and efficient sonic insulators. The transmission through a group of empty Cu cylinders decreases to background noise levels across a range of frequencies, which closely matches the predicted forbidden band based on calculations[50].

| Material | Frequency Band Gap | Design | References |
|-------------------|--------------------|-------------------------------------------------------------------------------------------------------------------------------------------------------------------------------------------------------------------------------------------------------------------------------------|------------|
| Rigid Metals | 164.9 % |  <p>An ultra-wide band gap (a BG of 165%) in the low-mid frequency range (from 250 Hz to 2500 Hz) can be achieved by the phononic crystal, which is generated by the rigid body resonances.</p> | [51] |
| vulcanized rubber | 22% |  | [52] |

| | | | |
|------------------------------|-----------------------|--|------|
| Silicon | 100% | | [28] |
| Copper | 100 kHz up to 2.5 MHz | | [53] |
| PVDF-polyvinylidene fluoride | 0.01–8.0 kHz | | [54] |

Table 2.1: shows design, material, and band gap frequency.

CHAPTER 3

Research Methodology

The key achievement lies in identifying the materials and designing the optimal phononic crystal structure to create a bandgap within the desired frequency range. In field of phononic crystal, many researcher use software for proposed models and results. But mostly worked at COMSOL MULTIPHYSICS Simulator because of the important feature.

This work preceded at COMSOL MULTIPHYSICS(registered) Simulator by using structural mechanics i7-8600 CPU, with RAM 32 GB, @2.9 GHz 64bit operating system for designing and counting the study for plotting data. We take the wave vector along x-axis and frequency along y-axis. The dispersion of elastic wave represents as spotted lines.. Two dimensional in plane modes for any filling area by using silicon carbide phononic crystal for various plot like bandgap, eigenmode shape.

To assess the frequency response of a phononic crystal, it is necessary to analyze the periodic unit cell while applying Bloch periodic boundary conditions across a spectrum of wave vectors. It is adequate to examine a limited range of wave vectors that encompasses the boundaries of the irreducible Brillouin zone (IBZ). The specific shape of this initial design is not specific, as the primary goal is simply to achieve a band gap (BG), which can be accomplished by sharp edges. Initially the chamfer corner is design to obtained the acoustic band gap but it was not successfully computed to obtained acoustic gaps.

The initial designed phononic crystal unit cell consist of chamfer edges with air hole inclusion in the center. The unit cell consist of 4 μm of each side, and air hole has varying size as shown in fig 3-1 below

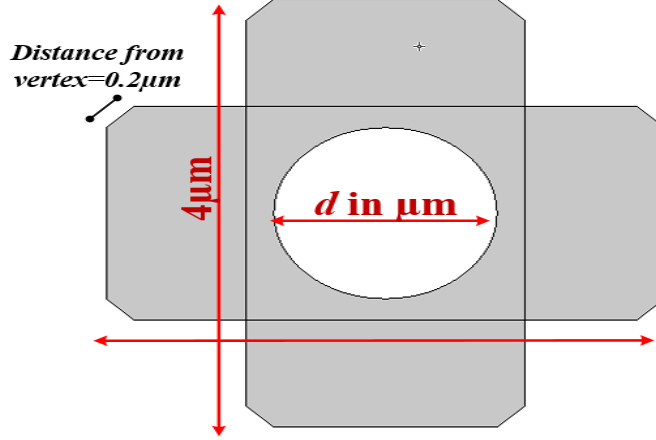


Figure 3.1:phononic crystal unit cell $4\mu\text{m} \times 4\mu\text{m}$ and chamfer vertex is $0.2\mu\text{m}$.

Then this initial designed phononic crystal unit cell is modified with sharp edges with varying air inclusion center hole. Thus, the propagation of waves through this geometry is governed by the elastic wave equation.

$$\rho u = (\lambda + 2\mu)\Delta u - \mu\nabla \times \nabla \times u$$

In this context, (\mathbf{r}) denotes the spatial displacement field, while $\mathbf{u}(\mathbf{r})$ indicates the acceleration, with \mathbf{r} representing the position vector. The material's density is given by ρ , and the Lamé coefficients are denoted by λ and μ . The symbols Δ and $\nabla \times$ refer to the 2D Laplacian and curl operators, respectively.

Utilize the Bloch–Floquet periodic boundary condition while sweeping the wave vector across the irreducible Brillouin zone (illustrated by solid lines in the BZ of the PnC unit cell structure where $\boldsymbol{\Gamma} = \mathbf{0}$) to obtain the band structure response. The equation is expressed as follows

$$u_{n+1}(r) = e^{ik.a}u_n(r)$$

In two dimensions, the wave vector is denoted as $\mathbf{k} = (k_x, k_y)$, while the lattice vector is represented by $a\mathbf{i} = (ax, ay)$, with the magnitudes of $\|ax\|$ and $\|ay\|$ both equal to a . Additionally, i denotes a complex number.

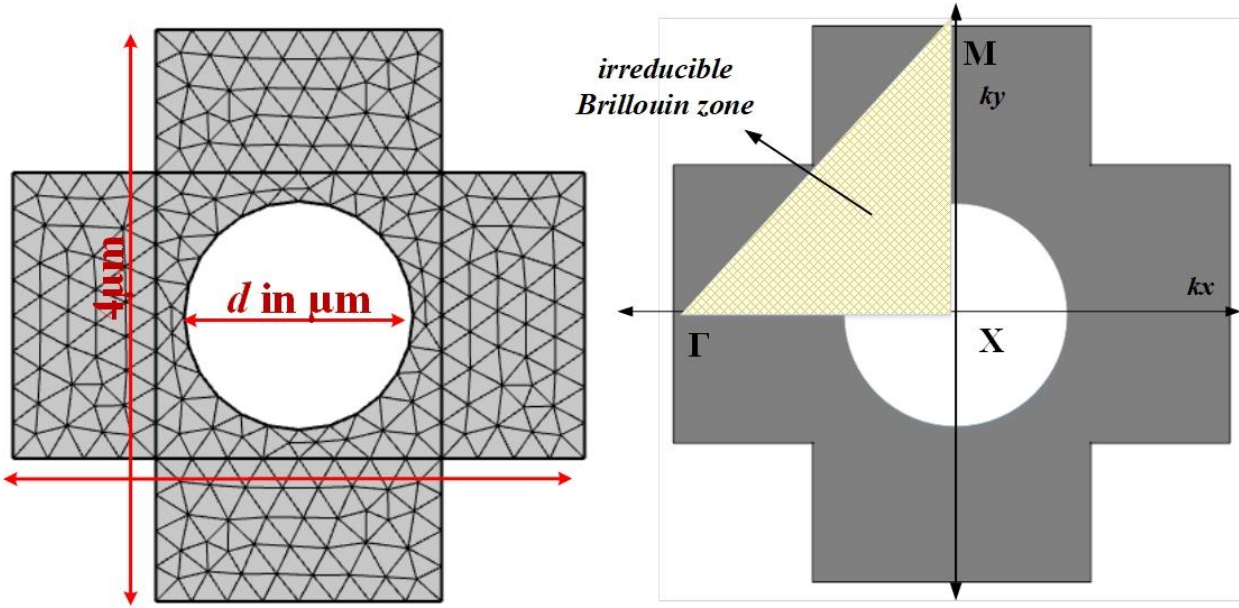


Figure 3.2: Mesh of proposed phononic crystal with sharp edges, and irreducible Brillouin zone of PnC for k parametric sweeping.

Limitations on the border displacements of the periodic structure are imposed by the Bloch boundary constraints (Floquet boundary conditions in one-dimensional systems). These conditions are applied to the left and right margins as well as the upper and lower margins of the unit cell. COMSOL Multiphysics supports this type of boundary condition, and because of their nature, a complex eigensolver is required. Nonetheless, the system of equations is Hermitian, ensuring that the eigenvalues are real, provided no damping is included in the model. COMSOL software simplifies this process by handling the calculations automatically.

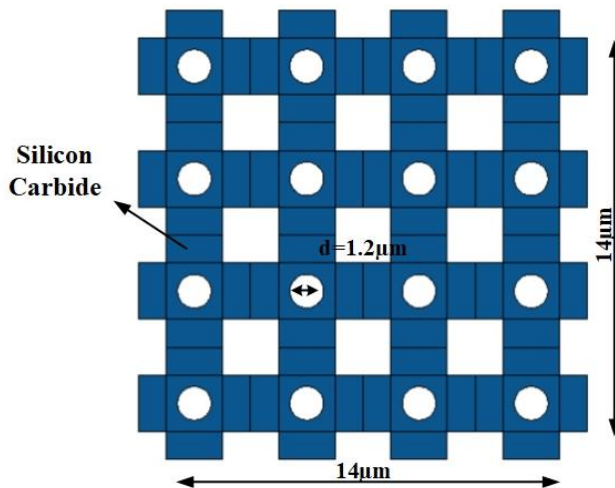
For the eigen solver analysis, we perform a parametric sweep over one parameter, k , ranging from 0 to 3. This range is divided into three segments: 0 to 1 covers the Γ -X edge, 1 to 2 spans the X-M edge, and 2 to 3 covers the diagonal M- Γ edge of the irreducible Brillouin zone (IBZ). The frequencies of wave propagation are plotted against k after we determine the lowest natural frequencies for each parameter. The plot reveals band gaps as regions with no wave propagation branches. Except for very complex unit cell models, this analysis is typically completed within short time. Thus, this method is an effective way to optimize for specific band gap locations or to maximize band gap width.

In this work three different materials silicon carbide, silicon nitride, and indium antimonide are employed to Phononic crystal and analyzed the bandgap, dispersion relations and their waves

mode shapes.

3.1 Silicon Carbide

At first the 4×4 array of PnC with radius of $0.6\mu\text{m}$ hole is taken for finding the dispersion curves, then increase air hole $0.7\mu\text{m}$, and $0.8\mu\text{m}$ and analyzed the elastic



waves curves.

Figure 3.3:Schematic diagram of a Silicon carbide PnC cell with lattice parameter $a = 4\mu\text{m}$, and Supercell model consisting of 4×4 cells with $1.2\mu\text{m}$ diameter hole.

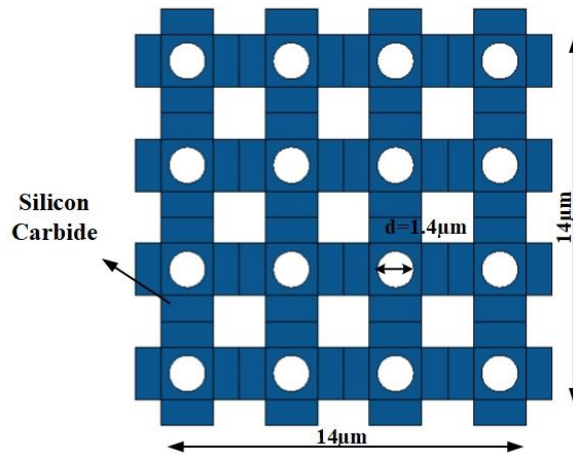


Figure 3.4:Schematic diagram of a Silicon carbide PnC cell with lattice parameter $a = 4\mu\text{m}$, and Supercell model consisting of 4×4 cells with $1.4\mu\text{m}$ diameter hole.

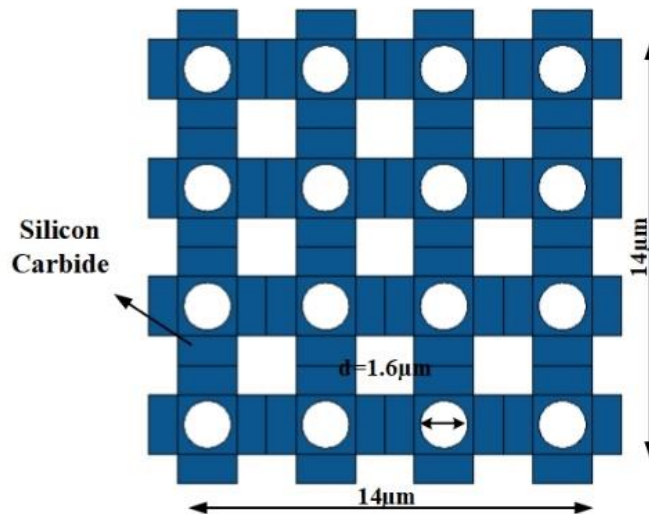


Figure 3.5:Schematic diagram of a Silicon carbide PnC cell with lattice parameter $a = 4\mu\text{m}$, and Supercell model consisting of 4×4 cells with $1.6 \mu\text{m}$ diameter hole.

| Property | Value | Unit |
|------------------------------------|--------|-------------------------------------|
| Density | 3216 | kg/m^3 |
| Young's modulus | 748E9 | Pa |
| Poisson's ratio | 0.45 | 1 |
| Coefficient of thermal expansion | 4.3E-6 | 1/K |
| Heat capacity at constant pressure | 690 | $\text{J}/(\text{kg}\cdot\text{K})$ |
| Relative permittivity | 9.7 | 1 |
| Thermal conductivity | 490 | $\text{W}/(\text{m}\cdot\text{K})$ |
| Density | 3216 | kg/m^3 |

Table 3.1:Properties of materials (SiC (6H) - Silicon carbide) used in the PnC structure.

3.2 Silicon Nitride

To analyzed the elastic waves and dispersion relation finite element simulation is also applied on the 4×4 array of PnC with air hole radius $0.6\mu\text{m}$ $0.7\mu\text{m}$, and $0.8\mu\text{m}$ of silicon nitride PnC structure.

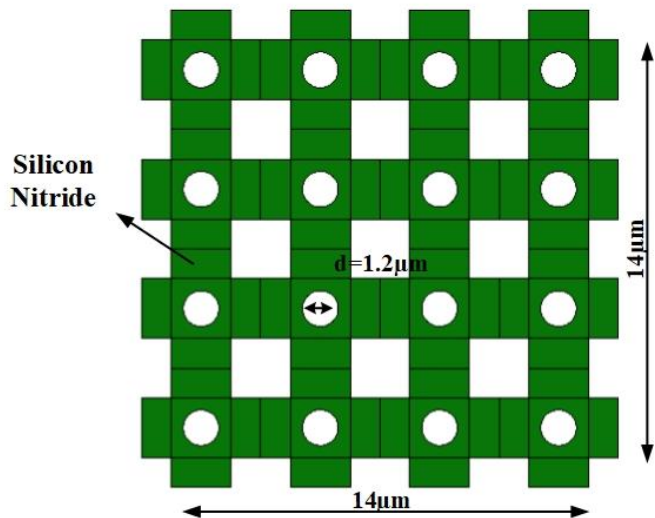


Figure 3.6:Schematic diagram of a Silicon Nitride PnC cell with lattice parameter $a = 4 \mu\text{m}$, and Supercell model consisting of 4×4 cells with $1.2 \mu\text{m}$ diameter hole.

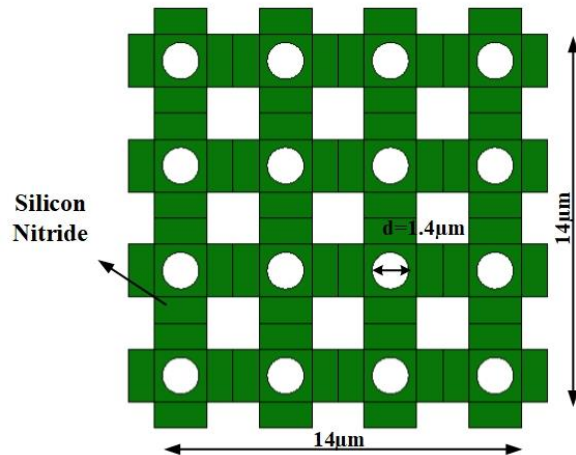


Figure 3.7:Schematic diagram of a Silicon Nitride PnC cell with lattice parameter $a = 4 \mu\text{m}$, and Supercell model consisting of 4×4 cells with $1.4 \mu\text{m}$ diameter hole.

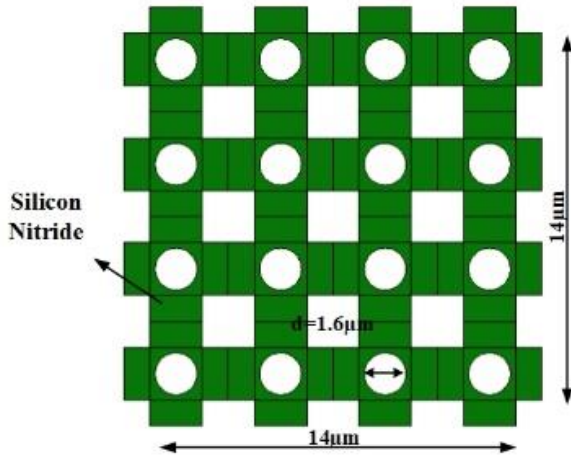


Figure 3.8:Schematic diagram of a Silicon Nitride PnC cell with lattice parameter $a = 4\mu\text{m}$, and Supercell model consisting of 4×4 cells with $1.6 \mu\text{m}$ diameter hole

| Property | Value | Unit |
|------------------------------------|-----------------|-------------------------------------|
| Density | 3100 | kg/m^3 |
| Young's modulus | $250\text{e}9$ | Pa |
| Poisson's ratio | 0.23 | 1 |
| Coefficient of thermal expansion | $2.3\text{e}-6$ | $1/\text{K}$ |
| Heat capacity at constant pressure | 700 | $\text{J}/(\text{kg}\cdot\text{K})$ |
| Relative permittivity | 9.7 | 1 |
| Thermal conductivity | 20 | $\text{W}/(\text{m}\cdot\text{K})$ |

Table 3.2:Properties of materials (Silicon Nitride) used in the PnC structure.

3.3 Indium Antimonide

To analyzed the elastic waves and dispersion relation finite element simulation is also applied on the 4×4 array of PnC with air hole radius $0.6\mu\text{m}$ $0.7\mu\text{m}$, and $0.8\mu\text{m}$ of indium antimonide PnC structure.

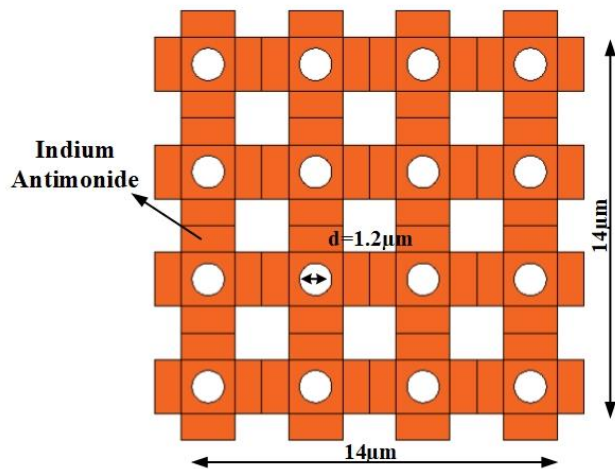


Figure 3.9:Schematic diagram of a Indium Antimonide PnC cell with lattice parameter $a = 4\mu\text{m}$, and Supercell model consisting of 4×4 cells with $1.2\mu\text{m}$ diameter hole.

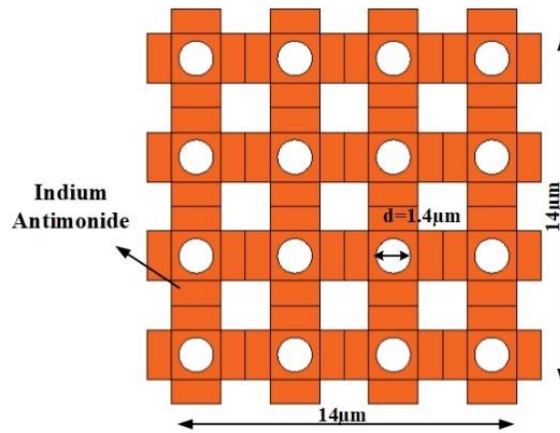


Figure 3.10:Schematic diagram of a Indium Antimonide PnC cell with lattice parameter $a = 4\mu\text{m}$, and Supercell model consisting of 4×4 cells with $1.4\mu\text{m}$ diameter hole.

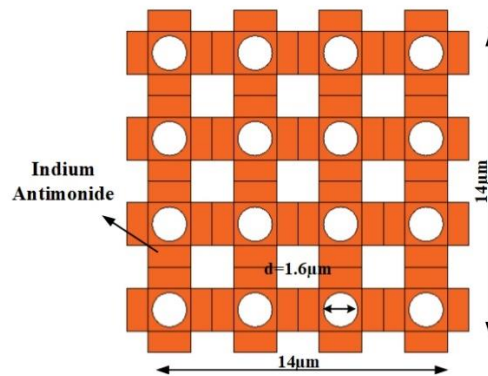


Figure 3.11:Schematic diagram of a Indium Antimonide PnC cell with lattice parameter $a = 4\mu\text{m}$, and Supercell model consisting of 4×4 cells with $1.6\mu\text{m}$ diameter hole.

| Property | Value | Unit |
|------------------------------------|--------------|-------------------|
| Density | 5770 | kg/m ³ |
| Young's modulus | 409e9 | Pa |
| Poisson's ratio | 0.35 | 1 |
| Coefficient of thermal expansion | 5.4e-6 | 1/K |
| Heat capacity at constant pressure | 200 | J/(kg·K) |
| Relative permittivity | 17.7 | 1 |
| Thermal conductivity | 18 | W/(m·K) |

Table 3.3:Properties of materials (Indium Antimonide) used in the PnC structure

CHAPTER 4

Results & Discussion

Simulated phononic band structure and dispersion curves for a phononic band gap material displayed in the figures featuring an air inclusion hole of radius($d/2$) $r=0.6\mu\text{m}$, $0.7\mu\text{m}$, $0.8\mu\text{m}$ employed to Silicon Carbide, Silicon Nitride, and indium antimonide.

We first investigated the in-plane mode phononic band gap of a MEMS (microelectromechanical systems) PnC with a square unit lattice where the parameters are $a_1=a_2=4\mu\text{m}$. This analysis was performed using the k-vector parametric solver in COMSOL Multiphysics® simulator through the Finite Element Analysis (FEA) method, which identified wide and complete band gaps. We applied Bloch wave boundary conditions within the first Brillouin zone, and the parametric steps are $[(\Gamma X) (k_x: 0 \text{ to } \pi \text{ while } k_y=0)]$, $[(\Gamma M) (k_y: 0 \text{ to } \pi \text{ while } k_x=\pi)]$, and $[(\Gamma M) (k_x \text{ and } k_y: 0 \text{ to } \pi)]$. The parametric sweep of k , ranging from 0 to 1, corresponds to the wave number within the irreducible Brillouin zone from Γ to X , as illustrated in band diagrams. For the two-dimensional PnC, the k-vector sweep spans the IBZ (irreducible Brillouin zone) segments Γ - X , X - M , and M - Γ , with the parameters 0-1, 1-2, and 2-3, respectively, as depicted in the figures below. The governing equation of bandgap ratio is given below

$$BG\% = \left(\frac{f_u - f_d}{\Delta f} \right) \%$$

Where $\Delta f = \left(\frac{f_u + f_d}{2} \right)$

Where f_u represent the upper and f_d represent lower bounds of the dispersion curves, While the wide and complete band gaps(BGs) are observed for all materials, indium antimonide exhibits the widest band gap.

Apply the Bloch–Floquet periodic boundary condition as varying the wave vector across the irreducible Brillouin zone (IBZ). So the Dispersion curve for the proposed Phononic crystals in irreducible Brillouin zone foundout through the FEA method are given below (The color lines indicate the elastic waves dispersion curves). At all frequencies outside the band gap, the periodic structure does not confine the vibrations. The corresponding responses are illustrated in the figures below.

The fig 4-1 represent the bands and dispersion relations of phononic crystal with chamfer edges.

From figure we see that there is no any bandgap is detected and some of the bands are interfering each other.

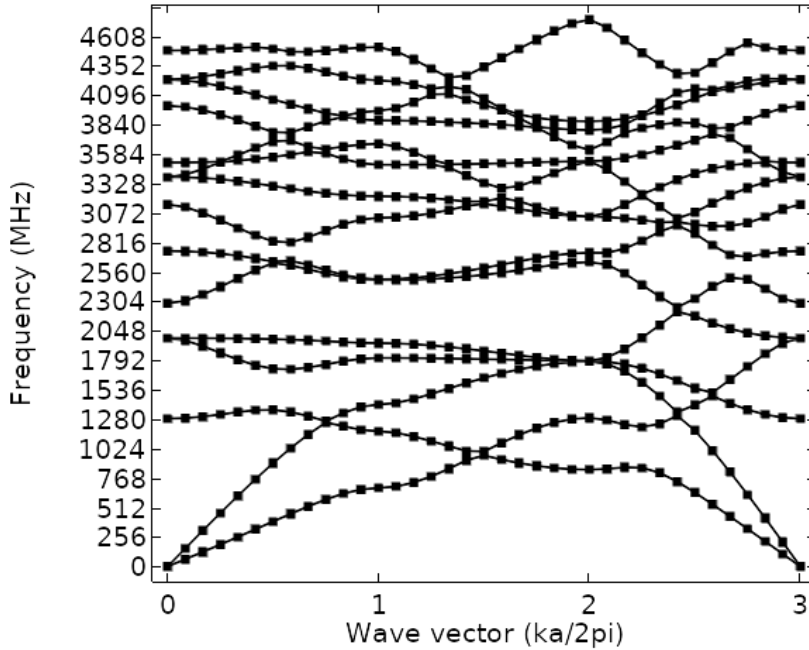


Figure 4.1: Illustration of bands and dispersion relations of phononic crystal with chamfer corner

Then the chamfer corner of phononic crystal is designed to sharp edges configure with air hole inclusions of radius $6\mu\text{m}$, $7\mu\text{m}$, and $8\mu\text{m}$ respectively. We see that the bandgap is created for $7\mu\text{m}$, and $8\mu\text{m}$ air hole inclusions.

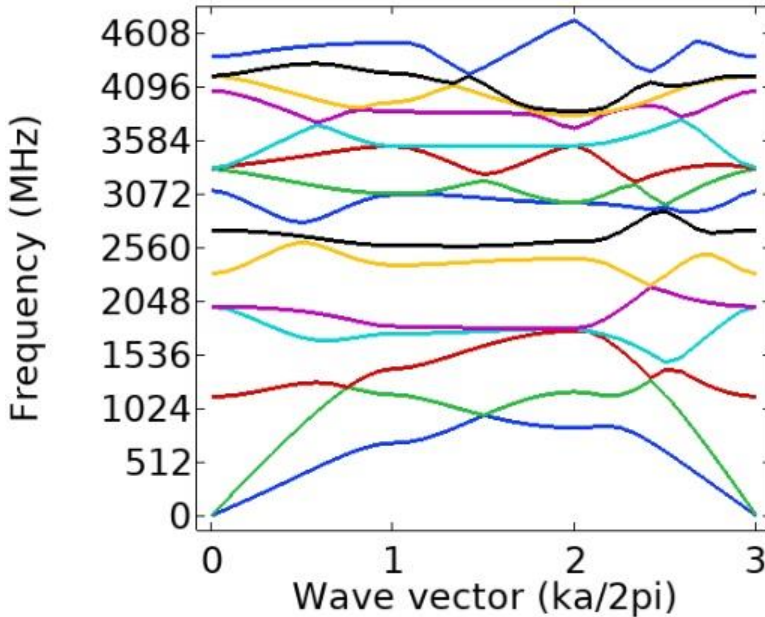


Figure 4.2: Dispersion curves and band structure of Silicon Carbide with $r=0.6\mu\text{m}$ hole

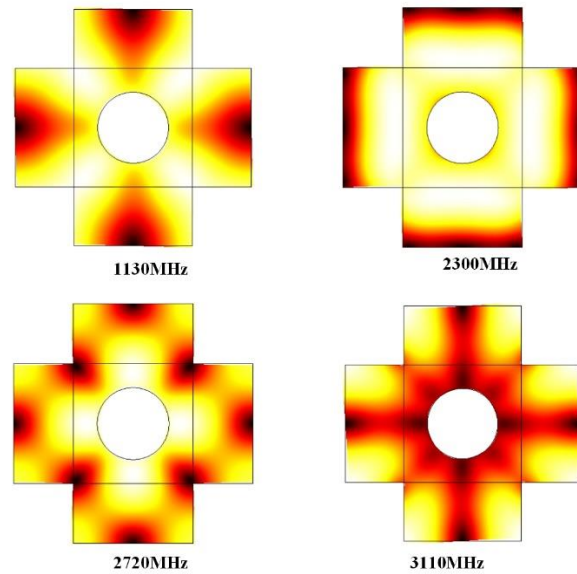


Figure 4.3:The eigenmode shapes of the first 4 frequency bands of the proposed PnC of Silicon Carbide with $r=0.6\mu\text{m}$ hole.

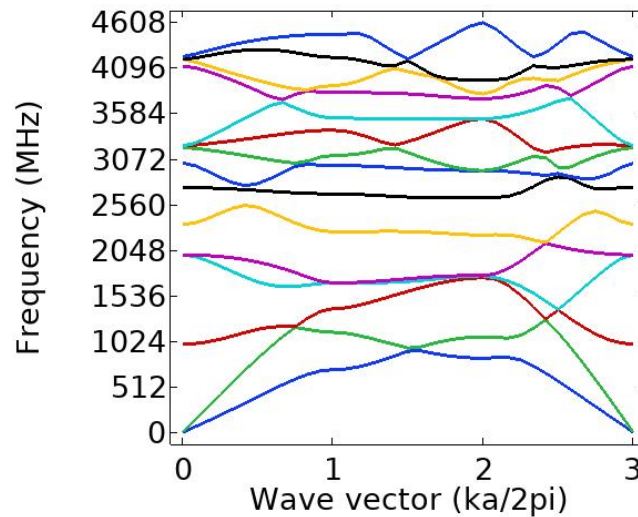


Figure 4.4:Dispersion curves and band structure of Silicon Carbide with $r=0.7\mu\text{m}$ hole.

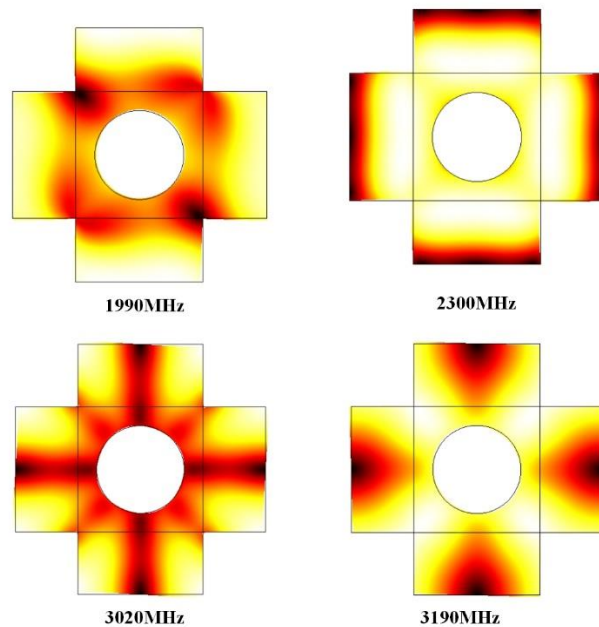


Figure 4.5:The eigenmode shapes of the first 4 frequency bands of the proposed PnC of Silicon Carbide with $r=0.7\mu\text{m}$ hole.

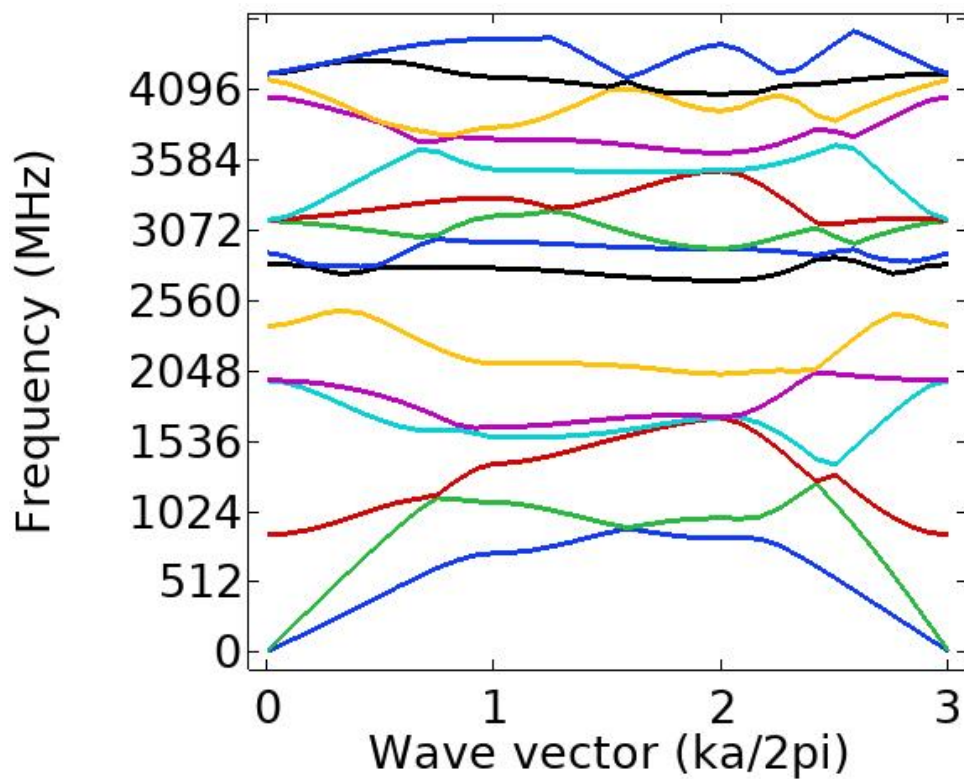


Figure 4.6:Dispersion curves and band structure of Silicon Carbide with $r=0.8\mu\text{m}$ hole

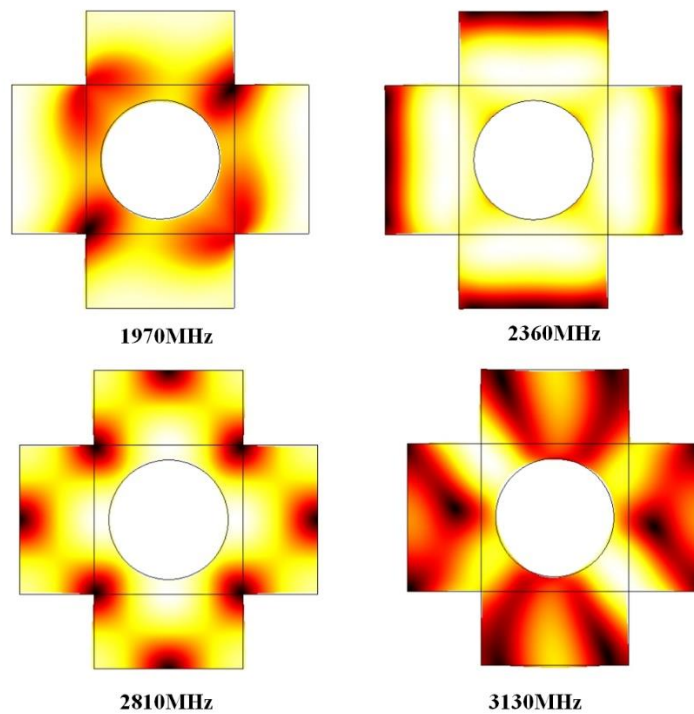


Figure 4.7:The eigenmode shapes of the first 4 frequency bands of the proposed PnC of Silicon Carbide with $r=0.8\mu\text{m}$ hole

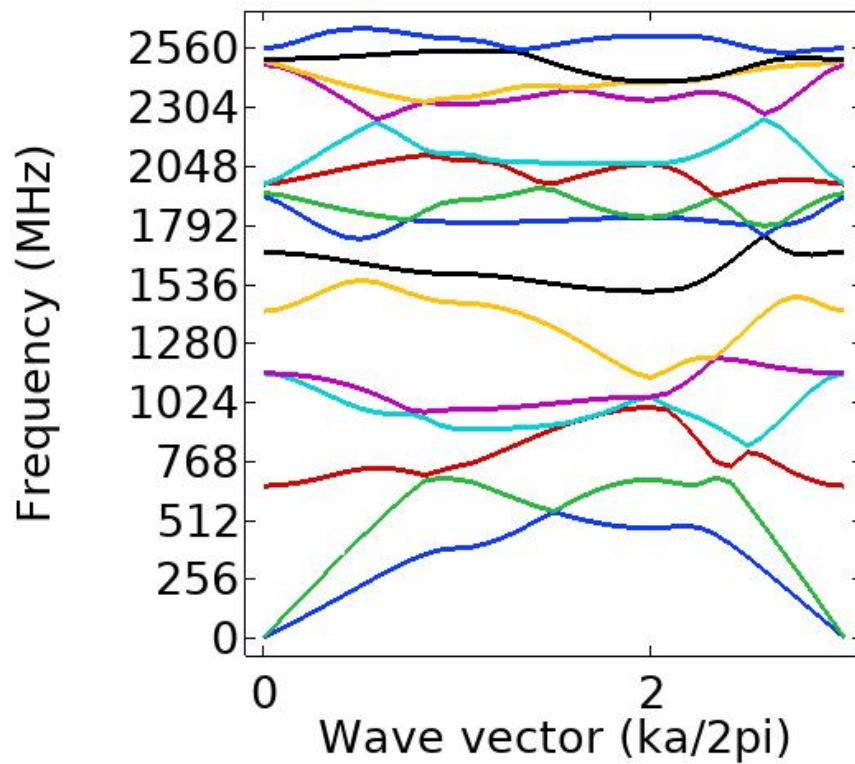


Figure 4.8:Dispersion curves and band structure of Silicon Nitride with $r=0.6\mu\text{m}$ hole

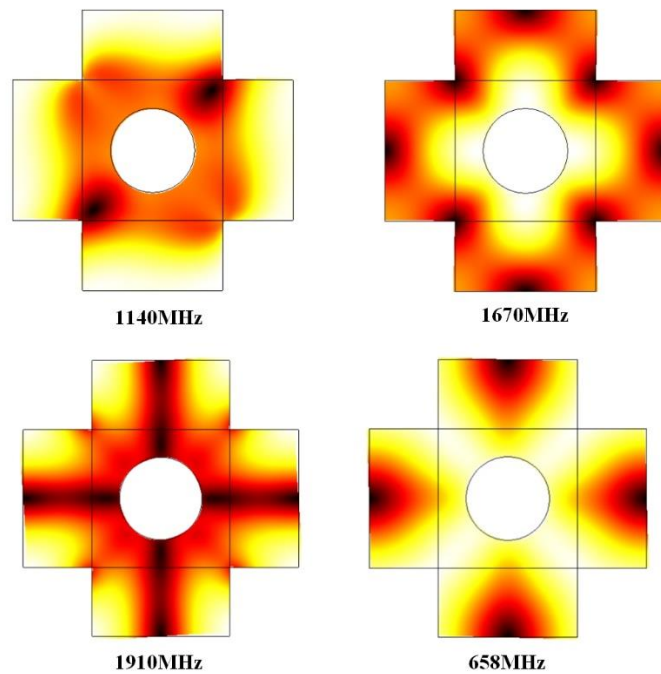


Figure 4.9:The eigenmode shapes of the first 4 frequency bands of the proposed PnC of Silicon Nitride with $r=0.6\mu\text{m}$ hole.

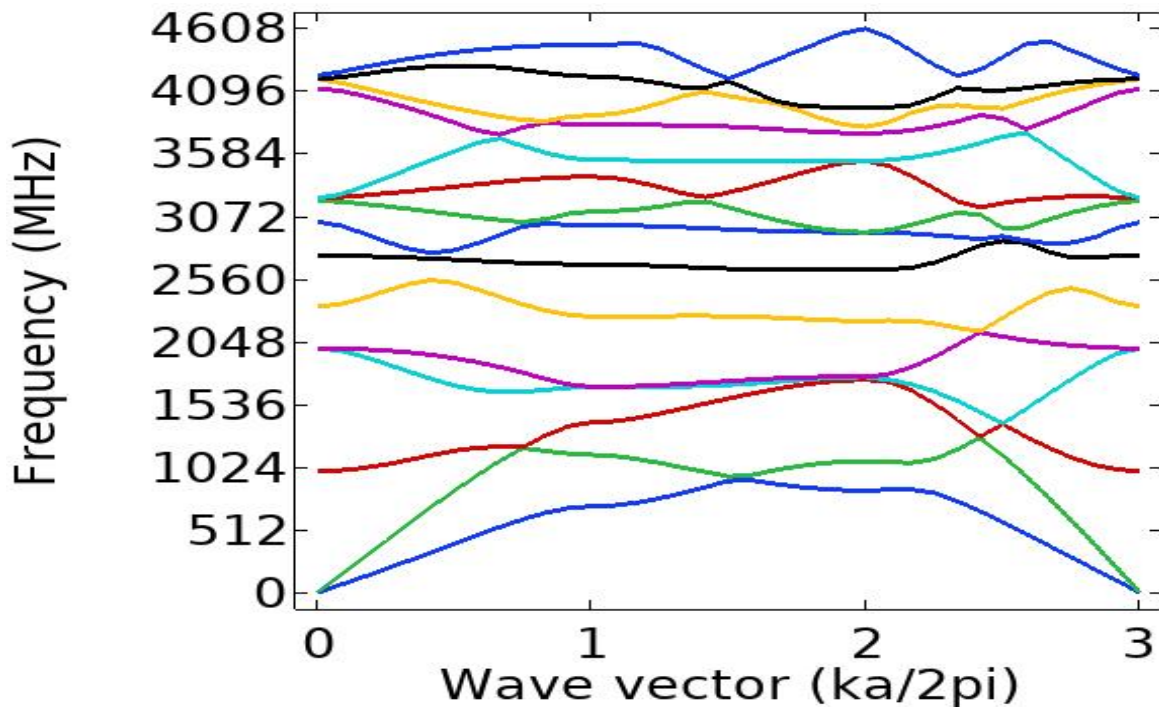


Figure 4.10:Dispersion curves and band structure of Silicon Nitride with $r=0.7\mu\text{m}$ hole

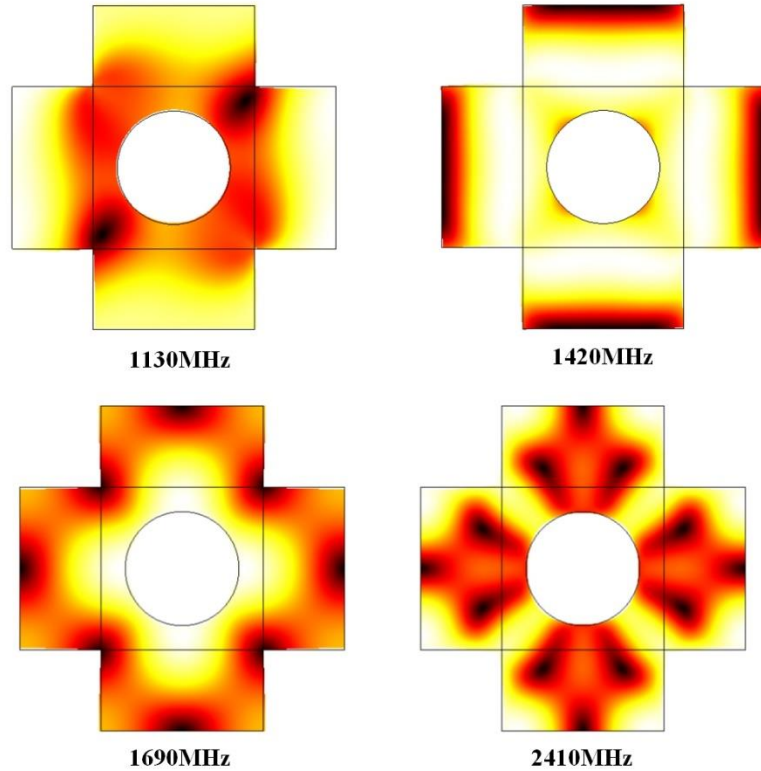


Figure 4.11: The eigenmode shapes of the first 4 frequency bands of the proposed PnC of Silicon Nitride with $r=0.7\mu\text{m}$ hole

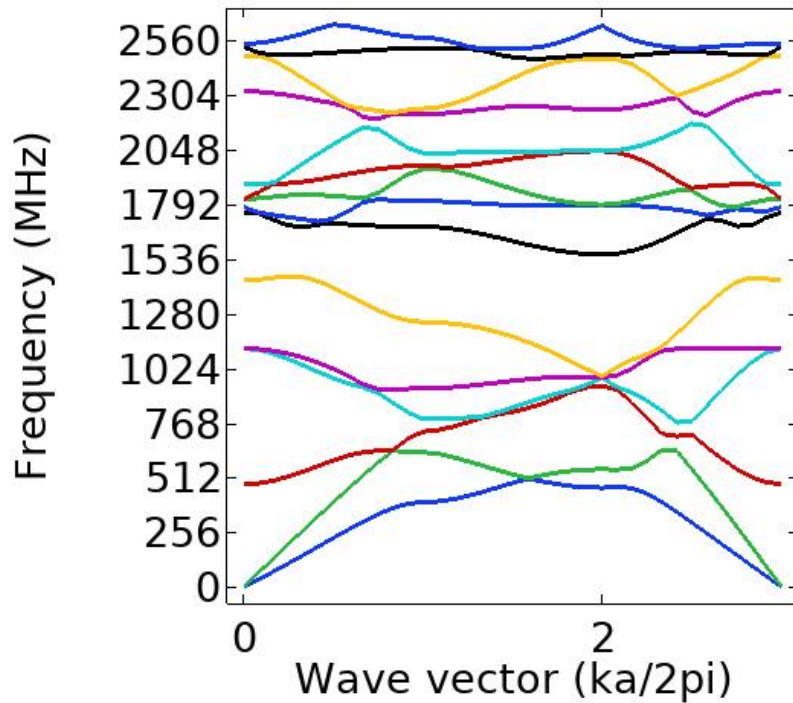


Figure 4.12: Dispersion curves and band structure of Silicon Nitride with $r=0.8\mu\text{m}$ hole

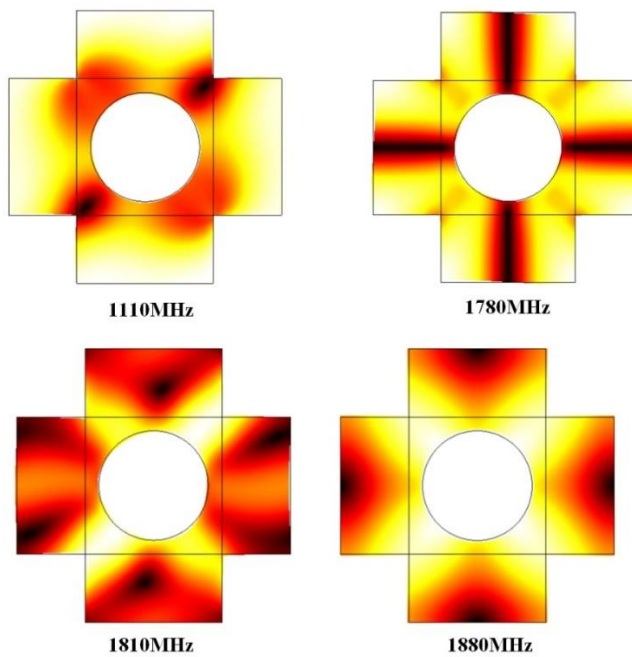


Figure 4.13:The eigenmode shapes of the first 4 frequency bands of the proposed PnC of Silicon Nitride with $r=0.8\mu\text{m}$ hole.

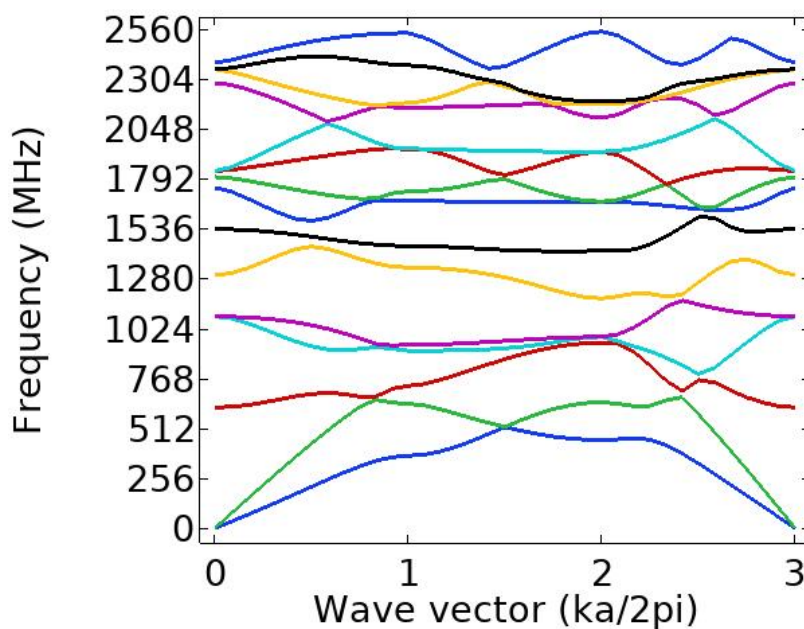


Figure 4.14:Dispersion curves and band structure of Indium antimonide with $r=0.6\mu\text{m}$ hole

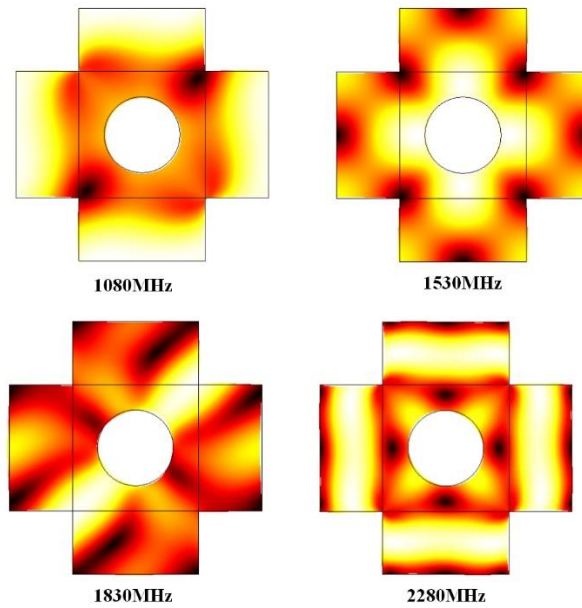


Figure 4.15: The eigenmode shapes of the first 4 frequency bands of the proposed PnC of Indium antimonide with $r=0.6\mu\text{m}$ hole.

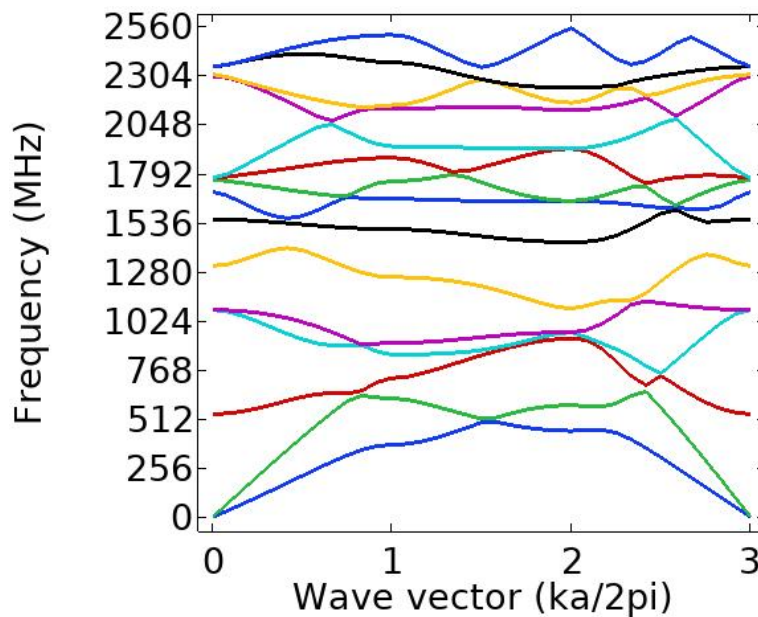


Figure 4. 16: Dispersion curves and band structure of Indium antimonide with $r=0.7\mu\text{m}$ hole

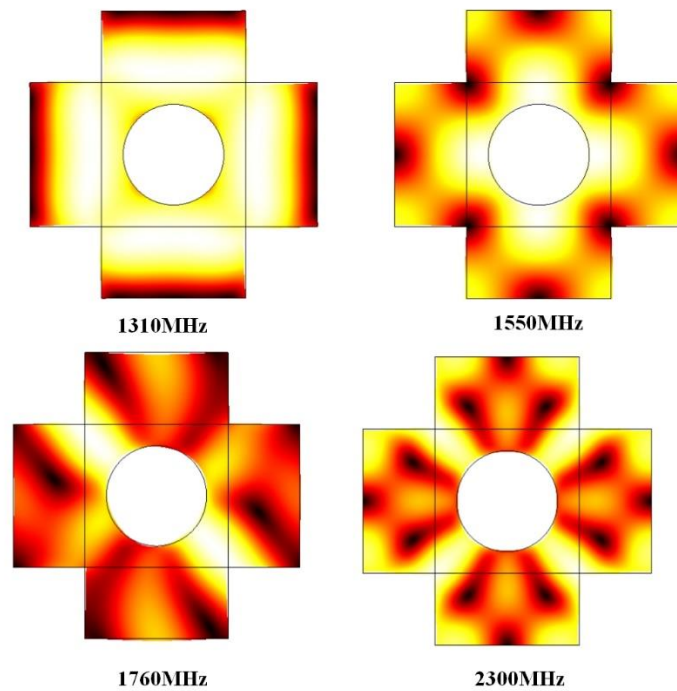


Figure 4.17:The eigenmode shapes of the first 4 frequency bands of the proposed PnC of Indium antimonide with $r=0.7\mu\text{m}$ hole.

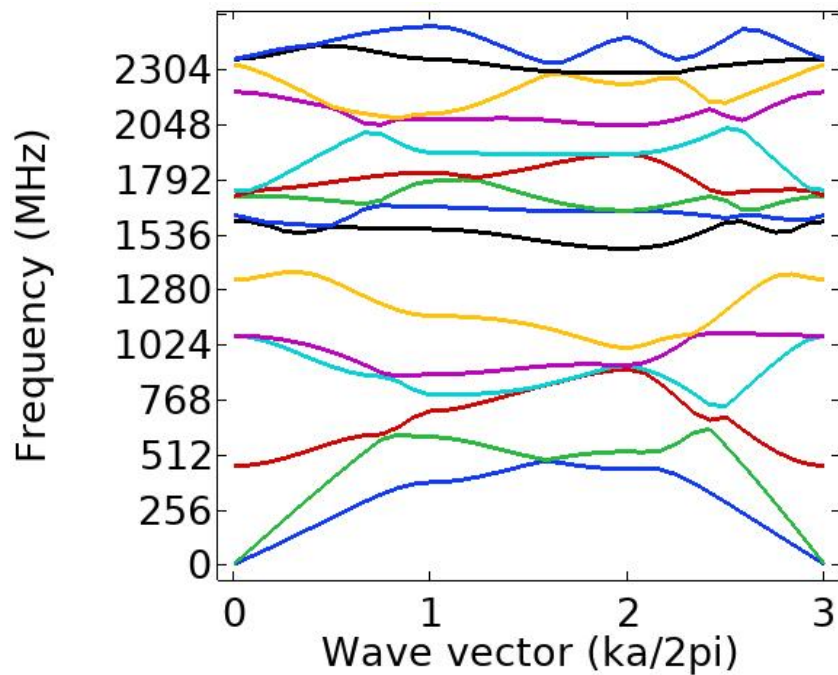


Figure 4.18:Dispersion curves and band structure of Indium antimonide with $r=0.8\mu\text{m}$ hole

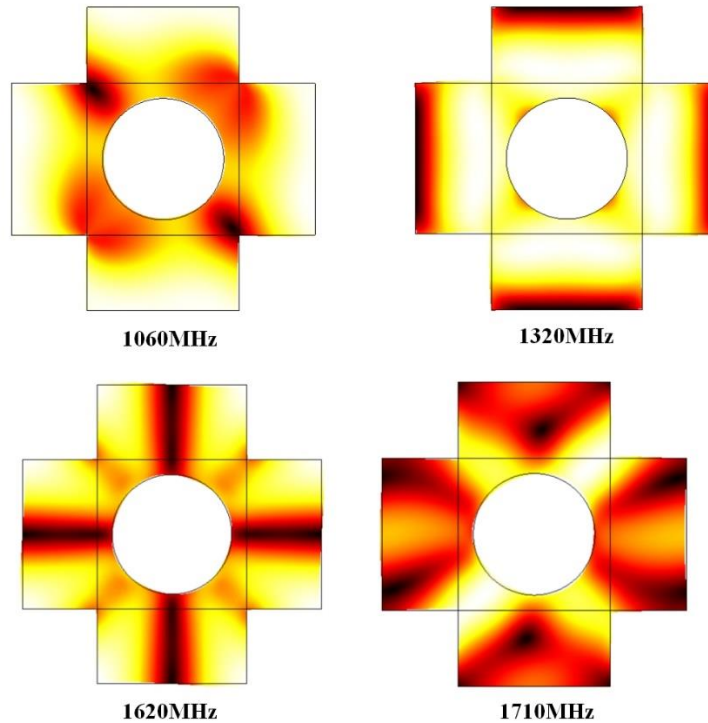


Figure 4.19: The eigenmode shapes of the first 4 frequency bands of the proposed PnC of Indium antimonide with $r=0.8\mu\text{m}$ hole.

The band gap ratio for silicon carbide, silicon nitride, and indium antimonide are also find in this work. When adjusting the size of air hole $6\mu\text{m}$ no bandgap is detected. The maximum bandgap is 260MHz is detected for silicon carbide at high frequency range, and 120MHz gap for indium antimonide at medium high frequency range.

| Silicon Carbide | | Upper limit | Lower limit | Frequency bandgaps | BG Ratio |
|------------------------|----------------|--------------------|--------------------|---------------------------|-----------------|
| | $6\mu\text{m}$ | No Gap | | | |
| | $7\mu\text{m}$ | 2640 | 2486 | 154 | 6% |
| | $8\mu\text{m}$ | 2745 | 2485 | 260 | 9.95% |
| Silicon Nitride | | | | | |
| | $6\mu\text{m}$ | No Gap | | | |
| | $7\mu\text{m}$ | 1519 | 1465 | 54 | 3.61% |
| | $8\mu\text{m}$ | 1558 | 1450 | 108 | 7.18% |
| Indium | | | | | |

| | | | | | |
|-------------------|-----|--------|------|-----|-------|
| Antimonide | 6μm | No Gap | | | |
| | 7μm | 1435 | 1404 | 31 | 2.18% |
| | 8μm | 1472 | 1352 | 120 | 8.5% |

Table 4.1: Upper and Lower frequency bands limits of three materials.

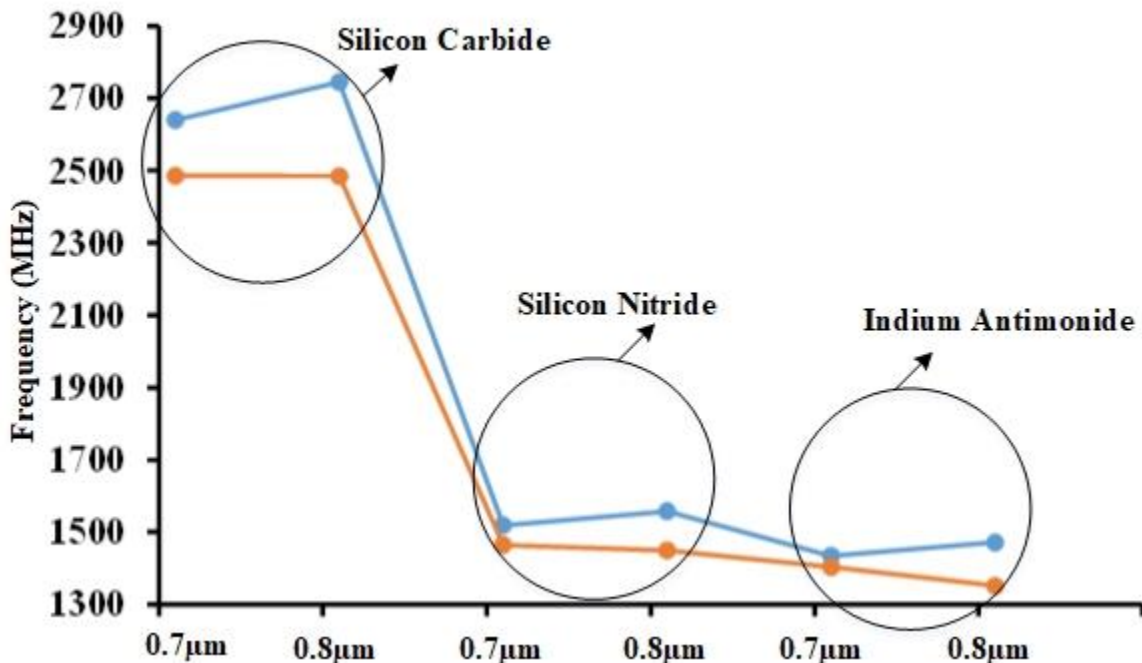


Figure 4.20: Illustration of band gaps of three materials with air hole inclusion of radium 0.7μm and 0.8μm

CHAPTER 5

Conclusion & Future Work

This study introduces a new method for optimizing the band gap and dispersion characteristics of In-plane mode two-dimensional phononic crystals. A novel phononic crystal design is proposed, and the behavior of acoustic/elastic waves within these two-dimensional phononic crystals (PnCs) is examined through periodic boundary Finite Element Analysis (FEA) simulations. The analysis reveals that adjusting the radius of the air inclusion holes in the phononic crystal can alter the forbidden and pass bands. The study explores how the absolute bandgap of the PnC varies with changes in the air inclusion and the material properties. Initially, the PnC unit cell, measuring $4\mu\text{m} \times 4\mu\text{m}$, featured chamfered edges but was later modified to include sharp edges with different air inclusion hole sizes at the center. Vibrational wave displacement and dispersion curves were analyzed for a 4×4 array of PnCs with air hole radii of $0.6\mu\text{m}$, $0.7\mu\text{m}$, and $0.8\mu\text{m}$. Three materials—silicon carbide, silicon nitride, and indium antimonide—were used in the PnC array. The results showed that a PnC with an $8\mu\text{m}$ air inclusion and silicon carbide material exhibited the widest bandgap, ranging from 2485 MHz to 2745 MHz. Additionally, it was observed that increasing the size of the air inclusion hole also expanded the bandgap.

5.1 Future work And Applications

One of the primary anticipated uses of PnC structures is in the creation of HF signal processing devices for wireless communication signals. Two established platforms for achieving these functions are bulk acoustic wave (BAW) systems (like FBARs) and surface acoustic wave (SAW) systems. Each platform offers distinct benefits and applications, making it valuable to explore phononic crystal implementations based on them. The fundamental components discussed in this book, including resonators and waveguides, can act as essential building blocks for more complex integrated acoustic systems. Devices used in wireless communications, such as filters, multi-plexers, and Demulti-plexers, can be realized and optimized through effective coupling of these basic components. Additionally, the ability to engineer dispersion in phononic crystal structures enables crucial functionalities like delay lines. Structures with band gaps may provide advantages such as reduced losses and enhanced control over component coupling within the system. Moreover, investigating PnC structural design for sensing applications is also worthwhile. These structures could be particularly useful for detecting targeted species in both gaseous and liquid environments, making them appealing for biosensing applications.

The manipulation of microfluidics is crucial for many fields, including creating lab-like environments for disease and toxin detection, as well as for drug delivery. To establish effective

procedures in these contexts, multiple functions—such as mixing, centrifuging, and dispensing liquids—are often necessary. These tasks require a significant concentration of power to be applied to the fluids and their droplets. Ultrasound presents an effective method for handling and manipulating liquids, enabling functionalities like mixing and nebulization. Generating the required power densities on a chip for selective liquid manipulation typically involves either high input power through various transducers or the efficient guiding of elastic waves to targeted locations. Phononic crystals, with their distinctive properties, are excellent candidates for these applications. Their inherent frequency-selective characteristics and guiding capabilities can significantly enhance lab-on-chip developments. Research by Reboud et al. has shown that phononic crystal structures can effectively manipulate liquids, demonstrating functions such as blood cells, as well as nebulization in micro-droplets. This initial exploration suggests that the potential for phononic crystal structures in on-chip microfluidic handling is only beginning to be realized, with greater advancements anticipated.

References

- [1] D. Leduc *et al.*, “Magnetic-Sphere-Based Phononic Crystals,” *Cryst. 2016, Vol. 6, Page 78*, vol. 6, no. 7, p. 78, Jul. 2016, doi: 10.3390/CRYST6070078.
- [2] S. Jiang, H. Hu, and V. Laude, “Ultra-Wide Band Gap in Two-Dimensional Phononic Crystal with Combined Convex and Concave Holes,” *Phys. status solidi – Rapid Res. Lett.*, vol. 12, no. 2, p. 1700317, Feb. 2018, doi: 10.1002/PSSR.201700317.
- [3] V. Laude, “Principles and properties of phononic crystal waveguides,” *APL Mater.*, vol. 9, no. 8, Aug. 2021, doi: 10.1063/5.0059035.
- [4] B. Graczykowski, N. Vogel, K. Bley, H. J. Butt, and G. Fytas, “Multiband Hypersound Filtering in Two-Dimensional Colloidal Crystals: Adhesion, Resonances, and Periodicity,” *Nano Lett.*, vol. 20, no. 3, pp. 1883–1889, Mar. 2020, doi: 10.1021/ACS.NANOLETT.9B05101/SUPPL_FILE/NL9B05101_SI_001.PDF.
- [5] A. Trzaskowska, P. Hakonen, M. Wiesner, and S. Mielcarek, “Generation of a mode in phononic crystal based on 1D/2D structures,” *Ultrasonics*, vol. 106, p. 106146, Aug. 2020, doi: 10.1016/J.ULTRAS.2020.106146.
- [6] Q. Li and M. Zhang, “Elastic Metamaterials of Hexagonal Unit Cells with Double-Cone Arms from Pentamode to Band Gap at Low Frequencies,” *Cryst. 2022, Vol. 12, Page 604*, vol. 12, no. 5, p. 604, Apr. 2022, doi: 10.3390/CRYST12050604.
- [7] S. Li, Y. Dou, L. Niu, S. Li, Y. Dou, and L. Niu, “Metal-Matrix Embedded Phononic Crystals,” *Photonic Cryst. - A Glimpse Curr. Res. Trends*, Oct. 2019, doi: 10.5772/INTECHOPEN.80790.
- [8] B. Jing-Fu, M. A. Khan, B. Fei-Hong, B. Jing-Fu, M. A. Khan, and B. Fei-Hong, “Phononic Crystal Resonators,” *Phonons Low Dimens. Struct.*, Nov. 2018, doi: 10.5772/INTECHOPEN.78584.
- [9] A. H. Aly, A. Mehaney, A. H. Aly, and A. Mehaney, “Phononic Crystals and Thermal Effects,” *Photonic Cryst. - A Glimpse Curr. Res. Trends*, Apr. 2019, doi: 10.5772/INTECHOPEN.82068.

- [10] M. I. Hussein, M. J. Leamy, and M. Ruzzene, “Dynamics of phononic materials and structures: Historical origins, recent progress, and future outlook,” *Appl. Mech. Rev.*, vol. 66, no. 4, Jul. 2014, doi: 10.1115/1.4026911/472528.
- [11] C. Croënne, E. J. S. Lee, H. Hu, ; J H Page, C. Crö, and J. H. Page, “Band gaps in phononic crystals: Generation mechanisms and interaction effects,” *AIP Adv.*, vol. 1, p. 41401, 2011, doi: 10.1063/1.3675797.
- [12] Z. ; Chen and Y. Wu, “Tunable Topological Phononic Crystals Item Type Article,” 2016, doi: 10.1103/PhysRevApplied.5.054021.
- [13] D. M. Profunser, E. Muramoto, O. Matsuda, O. B. Wright, and U. Lang, “Dynamic visualization of surface acoustic waves on a two-dimensional phononic crystal,” *Phys. Rev. B - Condens. Matter Mater. Phys.*, vol. 80, no. 1, p. 014301, Aug. 2009, doi: 10.1103/PHYSREVB.80.014301/FIGURES/6/MEDIUM.
- [14] N. Aravantinos-Zafiris, M. M. Sigalas, M. Kafesaki, and E. N. Economou, “Phononic crystals and elastodynamics: Some relevant points,” *AIP Adv.*, vol. 4, no. 12, Dec. 2014, doi: 10.1063/1.4904406/240363.
- [15] N. Wang *et al.*, “Micromechanical resonators based on silicon two-dimensional phononic crystals of square lattice,” *J. Microelectromechanical Syst.*, vol. 21, no. 4, pp. 801–810, 2012, doi: 10.1109/JMEMS.2011.2174416.
- [16] Z. Tian *et al.*, “Dispersion tuning and route reconfiguration of acoustic waves in valley topological phononic crystals,” *Nat. Commun. 2020* 111, vol. 11, no. 1, pp. 1–10, Feb. 2020, doi: 10.1038/s41467-020-14553-0.
- [17] W. He, L. Li, Z. Tong, H. Liu, Q. Yang, and T. Gao, “H-Shaped Radial Phononic Crystal for High-Quality Factor on Lamb Wave Resonators,” *Sensors 2023, Vol. 23, Page 2357*, vol. 23, no. 4, p. 2357, Feb. 2023, doi: 10.3390/S23042357.
- [18] M. Badreddine Assouar and M. Oudich, “Dispersion curves of surface acoustic waves in a two-dimensional phononic crystal,” *Appl. Phys. Lett.*, vol. 99, no. 12, Sep. 2011, doi: 10.1063/1.3626853/340702.

- [19] M. Maldovan and E. L. Thomas, “Simultaneous complete elastic and electromagnetic band gaps in periodic structures,” *Appl. Phys. B Lasers Opt.*, vol. 83, no. 4, pp. 595–600, Jun. 2006, doi: 10.1007/S00340-006-2241-Y/METRICS.
- [20] R. Chaunsali, F. Li, and J. Yang, “Stress Wave Isolation by Purely Mechanical Topological Phononic Crystals,” *Sci. Reports* 2016 61, vol. 6, no. 1, pp. 1–10, Aug. 2016, doi: 10.1038/srep30662.
- [21] F. Lucklum and M. J. Vellekoop, “Design and Fabrication Challenges for Millimeter-Scale Three-Dimensional Phononic Crystals,” *Cryst. 2017, Vol. 7, Page 348*, vol. 7, no. 11, p. 348, Nov. 2017, doi: 10.3390/CRYST7110348.
- [22] N. Aravantinos-Zafiris *et al.*, “View Online □ Export Citation CrossMark Phononic crystals and elastodynamics: Some relevant points Phononic crystals and elastodynamics: Some relevant points,” *AIP Adv.*, vol. 4, p. 124203, 2014, doi: 10.1063/1.4904406.
- [23] J. Liu *et al.*, “Q-Factor Enhancement of Thin-Film Piezoelectric-on-Silicon MEMS Resonator by Phononic Crystal-Reflector Composite Structure,” *Micromachines*, vol. 11, no. 12, pp. 1–13, Dec. 2020, doi: 10.3390/MI11121130.
- [24] D. Nardi *et al.*, “Probing thermomechanics at the nanoscale: Impulsively excited pseudosurface acoustic waves in hypersonic phononic crystals,” *Nano Lett.*, vol. 11, no. 10, pp. 4126–4133, Oct. 2011, doi: 10.1021/NL201863N/ASSET/IMAGES/LARGE/NL-2011-01863N_0006.JPG.
- [25] R. Anufriev, J. Maire, and M. Nomura, “Review of coherent phonon and heat transport control in one-dimensional phononic crystals at nanoscale,” *APL Mater.*, vol. 9, no. 7, Jul. 2021, doi: 10.1063/5.0052230/1064463.
- [26] T. Ampatzidis and D. Chronopoulos, “Mid-frequency band gap performance of sandwich composites with unconventional core geometries,” *Compos. Struct.*, vol. 222, p. 110914, Aug. 2019, doi: 10.1016/J.COMPSTRUCT.2019.110914.
- [27] S. Heiskanen, T. A. Puurtinen, and I. J. Maasilta, “Controlling thermal conductance using three-dimensional phononic crystals,” *APL Mater.*, vol. 9, no. 8, Aug. 2021, doi: 10.1063/5.0057385/1023828.

- [28] T. T. Wang, V. Laude, M. Kadic, Y. F. Wang, and Y. S. Wang, “Complex-Eigenfrequency Band Structure of Viscoelastic Phononic Crystals,” *Appl. Sci.* 2019, Vol. 9, Page 2825, vol. 9, no. 14, p. 2825, Jul. 2019, doi: 10.3390/APP9142825.
- [29] Y.-F. Wang, A. A. Maznev, V. Laude, V. J. Sanchez-Morcillo, V. Romero-Garcia, and L. M. Garcia-Raffi, “Formation of Bragg Band Gaps in Anisotropic Phononic Crystals Analyzed With the Empty Lattice Model,” *Cryst.* 2016, Vol. 6, Page 52, vol. 6, no. 5, p. 52, May 2016, doi: 10.3390/CRYST6050052.
- [30] Z. J. Shi, Y. S. Wang, and C. Z. Zhang, “Band structure calculation of scalar waves in two-dimensional phononic crystals based on generalized multipole technique,” *Appl. Math. Mech. (English Ed.)*, vol. 34, no. 9, p. 1123, Sep. 2013, doi: 10.1007/S10483-013-1732-6.
- [31] Z. Liu, C. T. Chan, P. Sheng, A. L. Goertzen, and J. H. Page, “Elastic wave scattering by periodic structures of spherical objects: Theory and experiment”.
- [32] R. Martínez-Sala, J. Sancho, J. V. Sánchez, V. Gómez, J. Llinares, and F. Meseguer, “Sound attenuation by sculpture,” *Nature*, vol. 378, no. 6554, p. 241, Nov. 1995, doi: 10.1038/378241A0.
- [33] J. P. Dowling, “Sonic band structure in fluids with periodic density variations,” 1992.
- [34] T. Vasileiadis *et al.*, “Progress and perspectives on phononic crystals,” *JAP*, vol. 129, no. 16, p. 160901, Apr. 2021, doi: 10.1063/5.0042337.
- [35] Y. Cang, Y. Jin, B. Djafari-Rouhani, and G. Fytas, “Fundamentals, progress and perspectives on high-frequency phononic crystals,” *J. Phys. D. Appl. Phys.*, vol. 55, no. 19, p. 193002, Jan. 2022, doi: 10.1088/1361-6463/AC4941.
- [36] Y. F. Wang, Y. Z. Wang, B. Wu, W. Chen, and Y. S. Wang, “Tunable and Active Phononic Crystals and Metamaterials,” *Appl. Mech. Rev.*, vol. 72, no. 4, p. 040801, Jul. 2020, doi: 10.1115/1.4046222.
- [37] S. H. Jo, H. Yoon, Y. C. Shin, W. Choi, B. D. Youn, and M. Kim, “L-shape triple defects in a phononic crystal for broadband piezoelectric energy harvesting,” *Nano Converg.*, vol. 9, no. 1, Dec. 2022, doi: 10.1186/S40580-022-00321-X.

- [38] S. H. Jo and B. D. Youn, “A Phononic Crystal with Differently Configured Double Defects for Broadband Elastic Wave Energy Localization and Harvesting,” *Cryst.* **2021**, Vol. 11, Page 643, vol. 11, no. 6, p. 643, Jun. 2021, doi: 10.3390/CRYST11060643.
- [39] F. He, N. Sheehan, X. Meng, S. R. Bank, R. L. Orbach, and Y. Wang, “Phonon-Phonon Quantum Coherent Coupling in GaAs/AlAs Superlattice”.
- [40] A. Erbes, W. Wang, D. Weinstein, and A. A. Seshia, “Acoustic mode confinement using coupled cavity structures in UHF unreleased MEMS resonators,” *Microsyst. Technol.*, doi: 10.1007/s00542-018-4118-5.
- [41] A. Scherer, Y. Xu, A. Yariv, and R. K. Lee, “Coupled-resonator optical waveguide: a proposal and analysis,” *Opt. Lett.* Vol. 24, Issue 11, pp. 711-713, vol. 24, no. 11, pp. 711–713, Jun. 1999, doi: 10.1364/OL.24.000711.
- [42] M. Kalderon, A. Paradeisiotis, and I. Antoniadis, “2D Dynamic Directional Amplification (DDA) in Phononic Metamaterials,” *Mater.* **2021**, Vol. 14, Page 2302, vol. 14, no. 9, p. 2302, Apr. 2021, doi: 10.3390/MA14092302.
- [43] A. H. Orta and C. Yilmaz, “Inertial amplification induced phononic band gaps generated by a compliant axial to rotary motion conversion mechanism,” *J. Sound Vib.*, vol. 439, pp. 329–343, Jan. 2019, doi: 10.1016/J.JSV.2018.10.014.
- [44] S. Taniker and C. Yilmaz, “Phononic gaps induced by inertial amplification in BCC and FCC lattices,” *Phys. Lett. A*, vol. 377, no. 31–33, pp. 1930–1936, Oct. 2013, doi: 10.1016/J.PHYSLETA.2013.05.022.
- [45] M. I. Hussein and M. J. Frazier, “Metadamping: An emergent phenomenon in dissipative metamaterials,” *J. Sound Vib.*, vol. 332, no. 20, pp. 4767–4774, Sep. 2013, doi: 10.1016/J.JSV.2013.04.041.
- [46] A. Bacigalupo and L. Gambarotta, “Damped Bloch Waves in Lattices Metamaterials with Inertial Resonators,” *Procedia Eng.*, vol. 199, pp. 1441–1446, Jan. 2017, doi: 10.1016/J.PROENG.2017.09.374.

- [47] B. X. Wang, G. Duan, C. Xu, J. Jiang, W. Xu, and F. Pi, “Design of multiple-frequency-band terahertz metamaterial absorbers with adjustable absorption peaks using toothed resonator,” *Mater. Des.*, vol. 225, p. 111586, Jan. 2023, doi: 10.1016/J.MATDES.2023.111586.
- [48] G. Y. Li, Y. Zheng, and Y. Cao, “Tunable defect mode in a soft wrinkled bilayer system,” *Extrem. Mech. Lett.*, vol. 9, pp. 171–174, Dec. 2016, doi: 10.1016/J.EML.2016.06.005.
- [49] J. L. Yagüe, J. Yin, M. C. Boyce, and K. K. Gleason, “Design of Ordered Wrinkled Patterns with Dynamically Tuned Properties,” *Phys. Procedia*, vol. 46, pp. 40–45, Jan. 2013, doi: 10.1016/J.PHPRO.2013.07.043.
- [50] J. O. Vasseur *et al.*, “Phononic crystal with low filling fraction and absolute acoustic band gap in the audible frequency range: A theoretical and experimental study,” *Phys. Rev. E*, vol. 65, no. 5, p. 056608, May 2002, doi: 10.1103/PhysRevE.65.056608.
- [51] G. Wen, H. Ou, and J. Liu, “Ultra-wide band gap in a two-dimensional phononic crystal with hexagonal lattices,” *Mater. Today Commun.*, vol. 24, p. 100977, Sep. 2020, doi: 10.1016/J.MTCOMM.2020.100977.
- [52] Y. Sun *et al.*, “Band gap and experimental study in phononic crystals with super-cell structure,” *Results Phys.*, vol. 13, p. 102200, Jun. 2019, doi: 10.1016/J.RINP.2019.102200.
- [53] D. Tallarico and S. G. Haslinger, “Trapped Modes and Negative Refraction in a Locally Resonant Metamaterial: Transient Insights into Manufacturing Bounds for Ultrasonic Applications,” 2021, doi: 10.3390/app11167576.
- [54] S. Palaz, Z. Ozer, C. Ahundov, A. M. Mamedov, and E. Ozbay, “Multiferroic based 2D phononic crystals: Band structure and wave propagations,” *Ferroelectrics*, vol. 544, no. 1, pp. 88–95, 2019, doi: 10.1080/00150193.2019.1598193.